MICROCOPY RESOLUTION TEST CHART
NATIONAL BUREAU OF

Report No. 4230667

AD A074974

ASW SONAR
TECHNOLOGY REPORT

(NAVships
(Nav Sea)
P

INFORMAL REPORT ON
ACOUSTIC MEASUREMENTS AT
PEARL HARBOR NAVAL SHIPYARD

LEVEL II

D D C
RECEIVED
OCT 12 1979
E

ARTHUR D. LITTLE, INC.
CAMBRIDGE, MASSACHUSETTS

DEPARTMENT OF THE NAVY
NAVAL SHIP SYSTEMS COMMAND

1

ASW SONAR
TECHNOLOGY REPORT

6 INFORMAL REPORT ON
ACOUSTIC MEASUREMENTS AT
PEARL HARBOR NAVAL SHIPYARD.

SEP 26 1979

ARTHUR D. LITTLE, INC.
CAMBRIDGE, MASSACHUSETTS

12 82

DEPARTMENT OF THE NAVY
NAVAL SHIP SYSTEMS COMMAND

15 NØØØ24-67-C-1448

Project Serial Number S 27-20

Task 11684

11 30 JUNE 1967

TABLE OF CONTENTS

1

LIST OF FIGURES

LIST OF FIGURES (Continued)

LIST OF TABLES

I. SUMMARY

This report presents the results of acoustic measurements conducted at the Wet Test Slip of the Pearl Harbor Naval Shipyard in March, 1967. The measurements included sound velocity profiles, bottom reflection loss, bottom cores, and ambient noise. The work was done to establish procedures useful in obtaining the types of acoustic information that will be required in shipyard locations for the SACS program, and to aid in selecting a location at Pearl Harbor for an interim SACS facility.

The following are the principal results and conclusions drawn:

(1) Velocity gradients occurring in the upper 10 to 20 ft. of water in the Wet Test Slip could interfere with source level measurements for a shallow transducer. However, no adverse effects should be experienced in range and bearing calibration at normal depth.

(2) Core analyses and porosity of the bottom material were obtained from cores taken by NAVOCEANO. A report on the cores is contained in the Appendix.

(3) Bottom reflection loss in the Wet Test Slip appears to be about what would be predicted based upon the core samples. However, variability of the bottom-loss measurements brings into serious question the adequacy of the approach utilized. Alternative approaches requiring further consideration are suggested.

(4) Snapping shrimp appear to be a primary source of ambient noise, which one measurement indicated to be about -19 db re 1μbar/Hertz at 6.5 kHz.

II. INTRODUCTION

NAVSHIPS, Code 1622D, is carrying out a project to improve the transducer measurements and calibration facilities at the Boston, Mare Island, and Pearl Harbor Naval Shipyards. Under this project, a Scientific Atlanta transducer calibration system will be provided at each of the three yards. Assisting Code 1622D, the Defense Research Laboratory (DRL) and Stanford Research Institute are making measurements at each facility to obtain data on environmental and acoustic characteristics. These data will aid in providing a sound basis for utilizing the calibration system and for determining the influence of particular characteristics of each site on the potential accuracy of transducer calibrations.

The transducer calibration facility at Pearl Harbor is located in the Wet Test Slip, which was originally excavated and dredged to accommodate floating drydocks. For a SACS facility located within the

-1-

boundaries of a shipyard, the dimensions of the Test Slip typify what could be expected to be available or could reasonably be achieved by excavation and dredging.

Since the information required for the transducer calibration facility was similar to that which would be required if the same location were being surveyed to determine its suitability for a SACS facility, it was decided to consider the potential value of participation by SACS personnel in this operation. A meeting among representatives of Code 1622D, Code 1622J, DRL, and ADL was held in Washington, 12 January 1967, to consider this question in detail. As a result of that meeting, it was decided to undertake a joint effort for the measurements to be made at Pearl Harbor. The principal reasons for doing so were:

(1) Without interfering with the original purposes, the measurements could be made so as to have maximum utility for SACS.

(2) Additional measurements of particular interest to SACS, alone, could be made by only a marginal increase in the effort.

(3) Valuable experience would be gained in carrying out an acoustic's survey operation for SACS within a shipyard.

(4) Sufficient information might be gained, at low cost, to provide a basis for selecting a location at Pearl Harbor for an interim SACS facility.

Accordingly, a measurements program was planned and carried out on this basis. It was conducted at the Pearl Harbor Naval Shipyard by personnel of Code 1622D, Code 1622J, DRL, SRI, and ADL during the period 6 March through 16 March 1967.

III. WET TEST SLIP ENVIRONMENT

The Wet Test Slip is located in the westerly part of the shipyard between the marine railway and drydock No. 3. Its general location is shown in Figure 1 and a plan view giving additional detail is shown in Figure 2. The area illustrated is used exclusively for activities associated with transducer measurements and calibration. There is an area dredged to a depth of about 50 ft. which is 100 ft. wide and 600 ft. long, but the transducer calibration utilizes only a small portion of this at the south end of the Test Slip. (For clarity and convenience of description, it is assumed that the long axis lies nominally in a north-south direction.)

A transducer mounting spindle is located at the end of a concrete platform on the west side of the Slip. A wire rope, 8 to 10 ft. above the water, is suspended between the platform and a concrete piling on the east

-2-
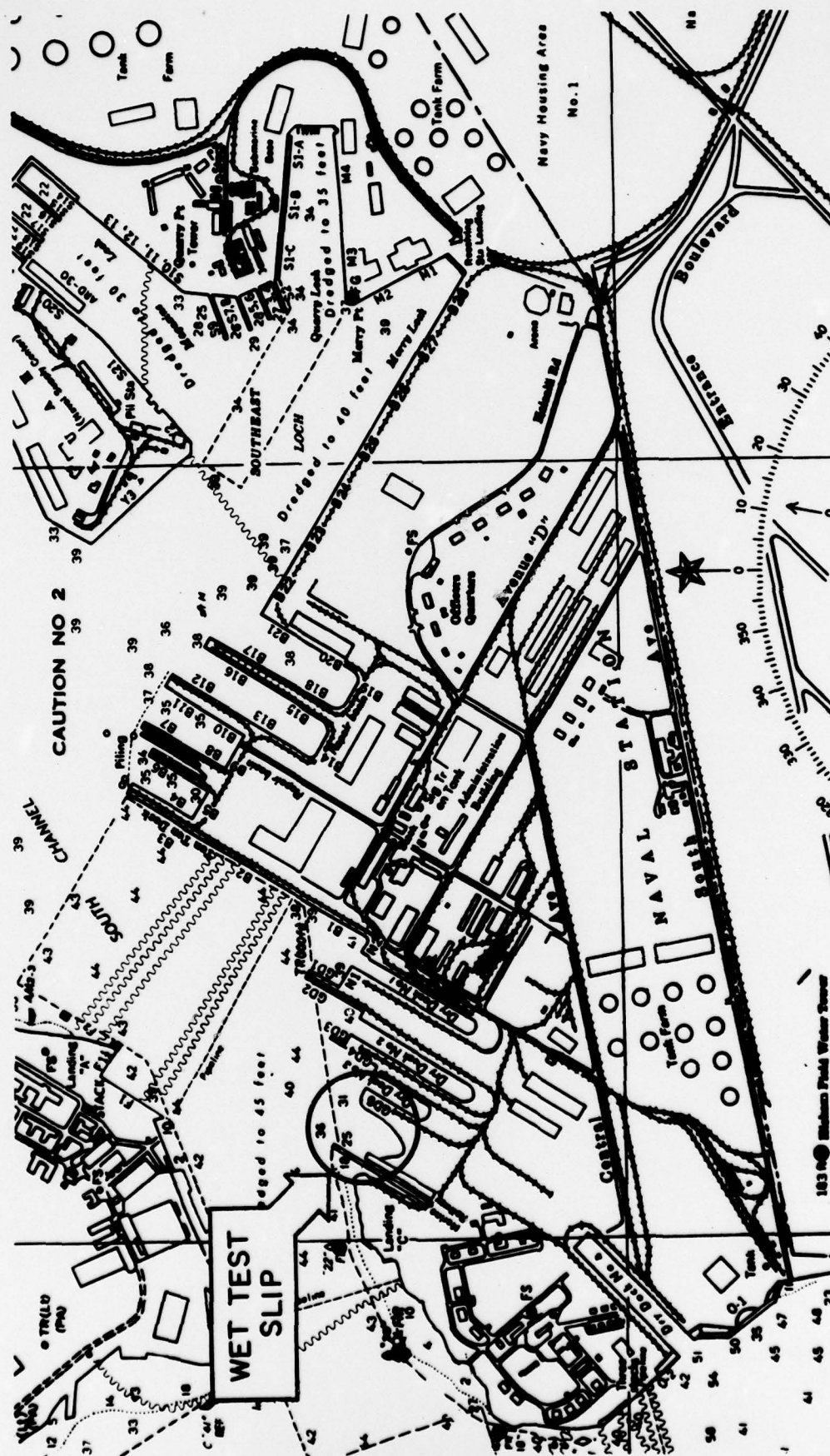
WET TEST SLIP LOCATION
PEARL HARBOR NAVAL SHIPYARD

FIGURE 1

-3-
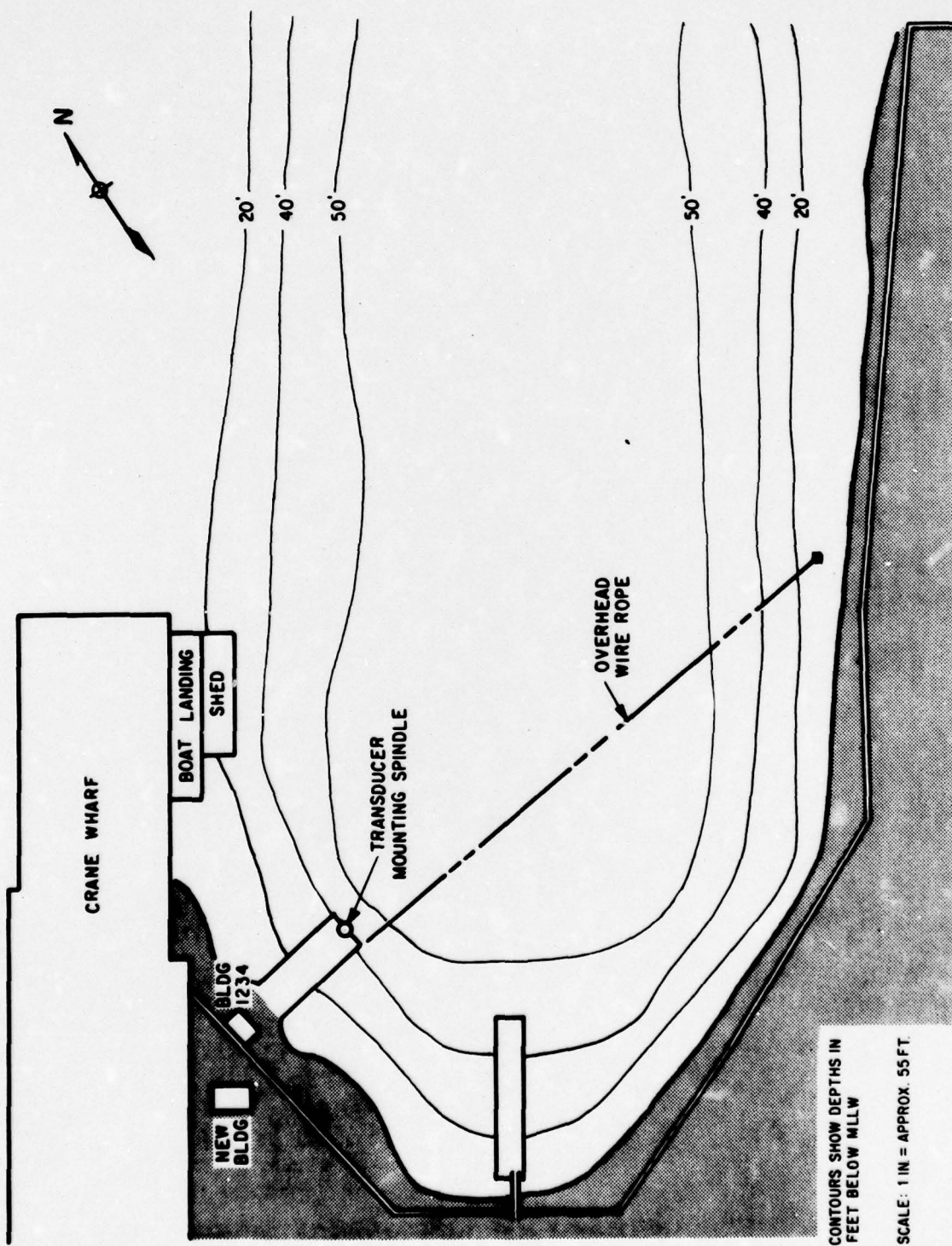
WET TEST SLIP
PEARL HARBOR NAVAL SHIPYARD
FIGURE 2

CONTOURS SHOW DEPTHS IN
FEET BELOW MLLW

SCALE: 1 IN = APPROX. 55 FT.

-4-

side of the Slip. For most of its length the wire rope is above water that is 50 ft. deep. Hydrophones are attached to trolleys on this wire and moved to desired locations with respect to the transducer spindle.

Building 1234 is a small, concrete block building housing the transmitter and presently-available instrumentation for conducting transducer calibrations. A new, semi-portable building has recently been moved into the location shown and will be used to house the Scientific Atlanta transducer calibration systems.

During the test period (6 March - 16 March) there was a generally high level of shipyard activity within the immediate vicinity of the Test Slip. Overhaul work was being conducted at the marine railway and in dry-dock No. 3. Sources of electrical noise, such as DC motor drives and welding equipment, were evident in the electromagnetic interference, and grounding problems were encountered with the instrumentation. Other sources of interference, such as ships' sonars and radars, were also noticeably active.

Due to its configuration, there is no net flow of water through the Test Slip. In spite of this, local conditions contribute to a surprisingly active fluctuation of water currents, particularly on the surface. The prevailing winds are northerly or northeasterly, setting up surface currents which carry in drift wood, trash, and miscellaneous organic material from vegetation. In addition, appreciable oil slicks are occasionally carried into the Slip. The tidal fluctuation of approximately two feet creates a twice-daily cycle of in-and-out-flow. Since the wet Slip opens directly into the channel carrying most of the Pearl Harbor traffic, the water surface is continually affected by the wakes of all types of vessels from small motor launches to large aircraft carriers.

Water and bottom conditions are affected by two storm drains and one sanitary sewer which empty directly into the Wet Test Slip. The surface water temperature and salinity can be temporarily affected by the storm drains. These carry rainfall from a surface area that is much larger than the water surface in the Slip itself. Hence, a 1-inch rainfall results, in effect, in several inches of rainwater dumping directly into the Slip.

For the most part weather conditions during the test period were dominated by Kona winds, which are a southerly flow that brings clouds, overcast, and rain, in contrast to the northeasterly trades which generally provide sunny, moderate conditions for the leeward side of the islands. Hence, temperature, wind direction, and rainfall were not typical of conditions prevailing here throughout most of the year.

IV. PROCEDURES AND RESULTS

A. SOUND VELOCITY PROFILES

Sound velocity profile measurements were made using a velocimeter mounted on a Boston Whaler supplied by the shipyard. Initially the measurements were made at 2-meter intervals from the surface to the bottom.

Inspection of the data showed that most of the velocity change occurred in the top six meters; therefore, the procedure was changed to reading the velocity at 1-meter intervals to a depth of six meters and at 2-meter intervals from there to the bottom. Depth determinations were made by means of a mechanical counter which measured the amount of cable paid out. Sound velocity measurements were made at the three locations shown in Figure 3 on the morning and afternoon on 7, 8, and 13 March 1967.

1. Results

The profiles observed at the three stations on 8 March are shown in Figure 4. These are also typical of the profiles occurring on 7 March. There is a positive gradient (of about 1/sec) down to a depth of approximately 10 ft. and a constant velocity from there to the bottom.

Figure 5 shows the profiles observed on 13 March. These followed a period of quite heavy rainfall, which apparently affected the sound velocity to a depth of about 20 ft. It should be noted that, because of two storm drains which empty into it, the amount of rainfall which ends up in the Wet Test Slip probably exceeds by a considerable quantity the amount which falls directly on its surface.

2. Analysis

If a uniform salinity is assumed from the surface to the bottom, the only way to account for the observed velocity profiles is with a cold surface layer. This is an unstable condition and cannot persist.

It is more reasonable to assume a uniform temperature with depth, which invokes a salinity controlled velocity profile. With a uniform temperature assumed, the salinity at 30 feet was calculated to be 33.4°/₀₀ on 8 March and 30.3°/₀₀ on 13 March. Considering the runoff into Pearl Harbor, and the tidal mixing through the harbor entrance, the 8 March salinity seems very consistent with the March mean surface salinity of 34.5% at Honolulu[*]. In light of the mixing it would be expected that conditions throughout the harbor might be quite uniform below a thin surface layer. It does not seem reasonable that the entire volume of the harbor could be diluted to the 30.3°/₀₀ computed for the 13 March deep water. Therefore, although a uniform temperature assumption works well on 8 March, it is not suitable for 13 March. The salinity profiles for 8 March were computed from the velocity profiles on the basis of the uniform temperature assumption.

Since the velocity below 23 feet showed little day to day change, and a gross change in salinity seems unlikely, we assumed (for 13 March) no temperature change below 23 feet, and a linear gradient to the surface. This distribution was chosen for simplicity, and to make the salinity at 20 feet constant between the two days. The 13 March salinity profiles

---

(*) Advance Copy - Appendix A - Review of Naval Shipyards with Respect to Suitability for SACS Facilities

-6-

N

CRANE WHARF

BOAT LANDING

SHED

TRANSDUCER
MOUNTING SPINDLE

A

20'
40'
50'

C

50'
40'
20'

BLDG
1234

NEW
BLDG

OVERHEAD
WIRE ROPE

B

CONTOURS SHOW DEPTHS IN
FEET BELOW MLLW
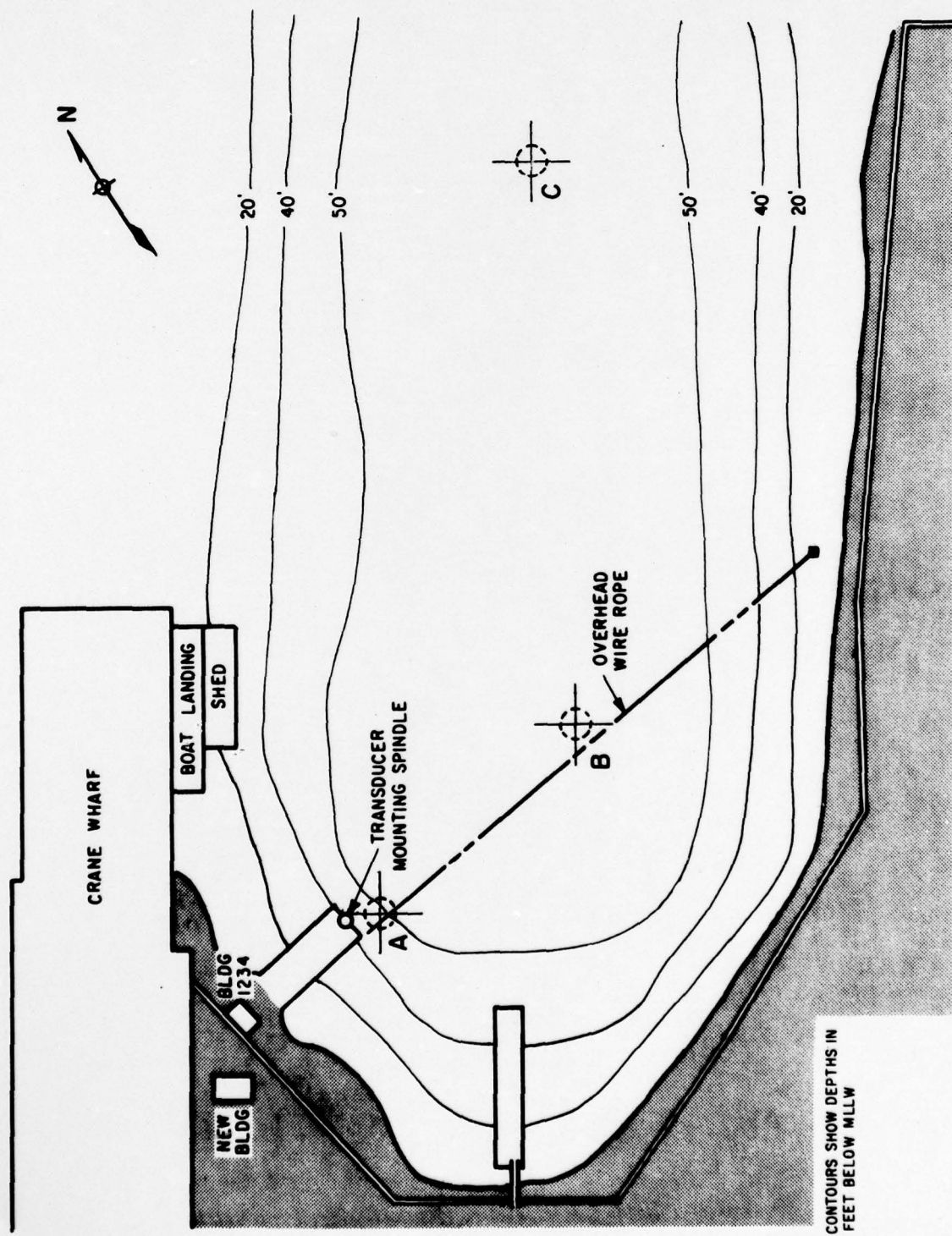
WET TEST SLIP
VELOCIMETER STATIONS
FIGURE 3

SOUND SPEED (ft./sec.)

STA. C

SOUND SPEED (ft./sec.)

STA. B

SOUND SPEED (ft./sec.)

STA. A

DEPTH (feet)
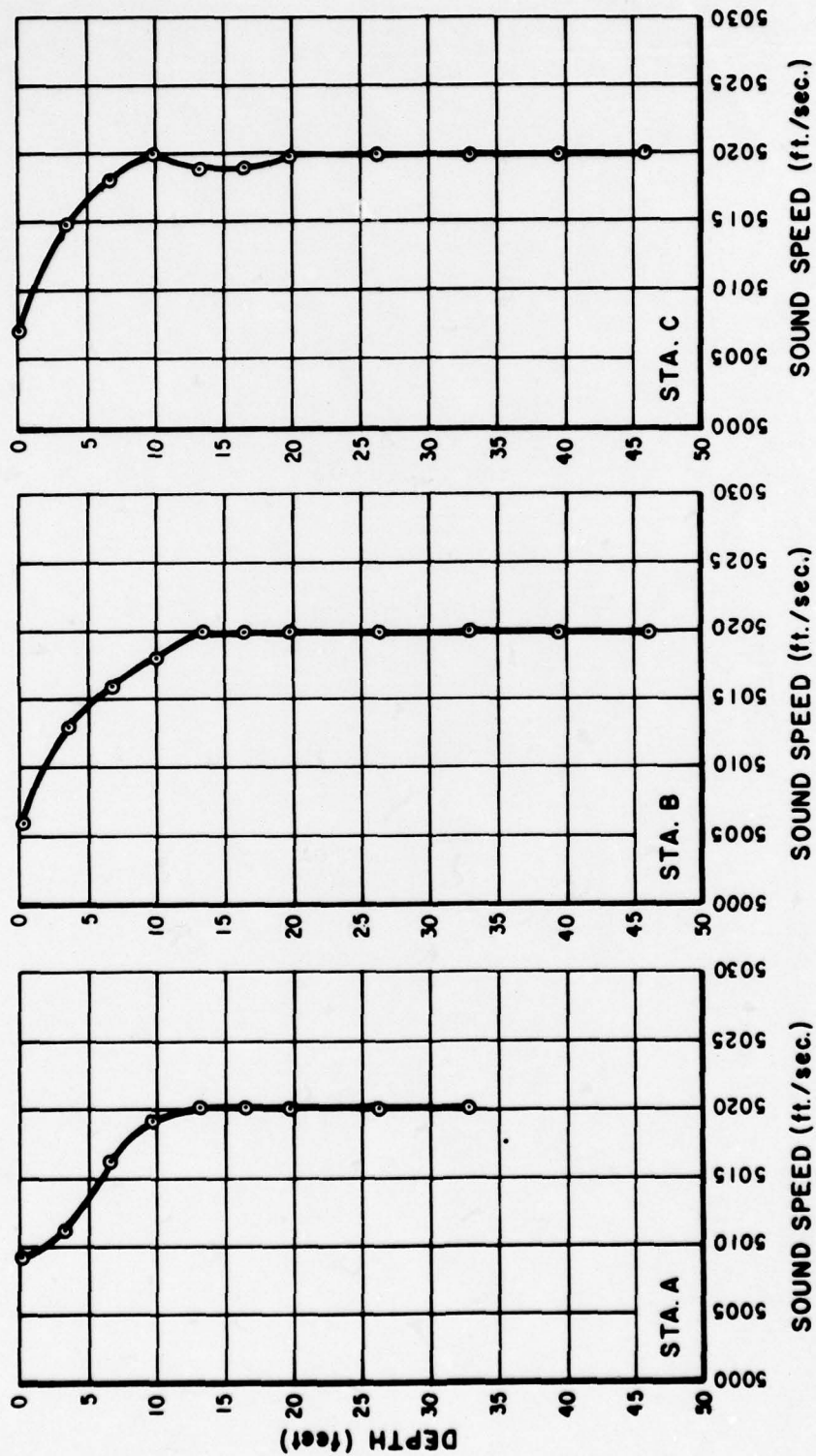
SURFACE TEMPERATURE = 75 F

PROFILES 8 MAR 1967

FIGURE 4
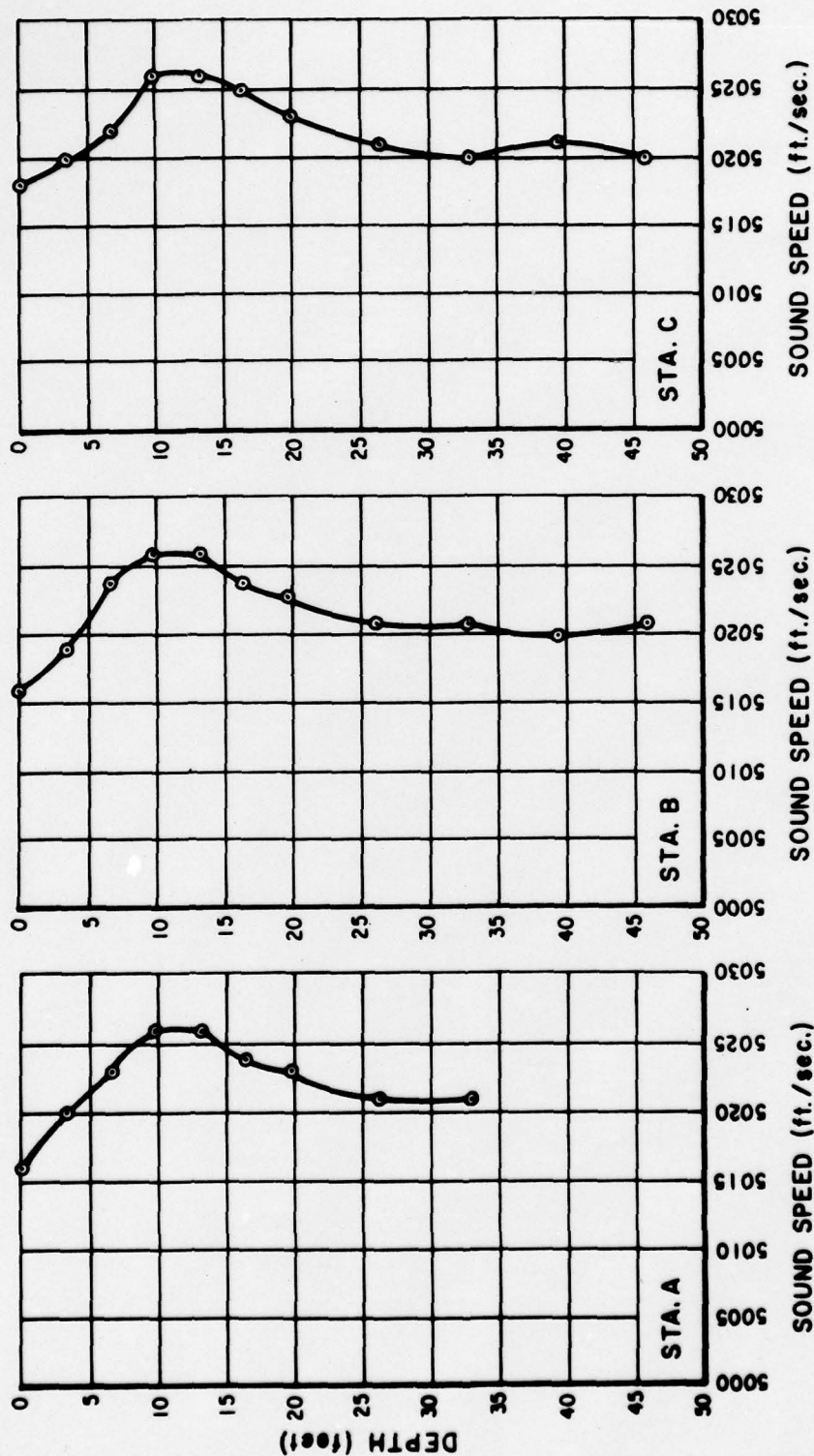
PROFILES 13 MAR 1967
FIGURE 5

SURFACE TEMPERATURE = 77.5 F

were computed from the velocity profiles using this assumed temperature distribution, and the results are shown in Figure 6.

A reasonably consistent picture of the processes which controlled the velocity profiles can be hypothesized. On 8 March a steady-state condition existed whereby fresh water was discharged (by sewer outfalls at the head of the Slip) which diffused downward and flowed outward over the surface of the uniformly mixed harbor water. This fresh water was at the same temperature as the harbor water resulting in isothermal conditions, and the observed salinity controlled velocity profile. Between 8 March and 13 March, the temperature and the quantity of fresh runoff increased markedly, increasing the surface temperature by 1.4°C and decreasing the salinity of the upper 20 feet by an average of nearly 0.5°/₀₀.

Along with heavy rains, we consider the large drainage area to account for temperature increase as well as quantity increase of the fresh water discharge. A larger drainage area in this case implies a greater distance travelled by the water, hence longer residence time on hot pavement before entrance to the storm sewers.

Velocimeter stations A and B are in close agreement with the above hypothesis. Station C does not fit as nicely (as is to be expected) due to its larger separation from the fresh water source, and its closer proximity to the open harbor. The assumed temperature profile probably does not fit the true conditions at station C as well as it does the conditions at A and B.

In any case, it appears that there was no mixed surface layer on either day, and that conditions were nearly uniform below 13 ± 1 feet on 8 March, and below 22 ± 1 feet on 13 March.

3. Conclusions

Assuming that the velocity profiles observed during this period are typical for the Wet Test Slip, we have examined whether these profiles would importantly affect its use as a calibration (or SACS-type) facility.

The observed conditions can be approximated by a positive gradient of $g = 1.0$/sec. overlying a layer of isovelocity water of sound speed 5020 feet/sec. Assume that a source is located midway between the surface and the top of the isovelocity layer. The limiting ray may be determined from:

$$d_L - d_s = \frac{C_v}{g} \left(\cos \phi_L - \cos \phi_s \right)$$

-10-

INFERRED SALINITY PROFILES
FIGURE 6
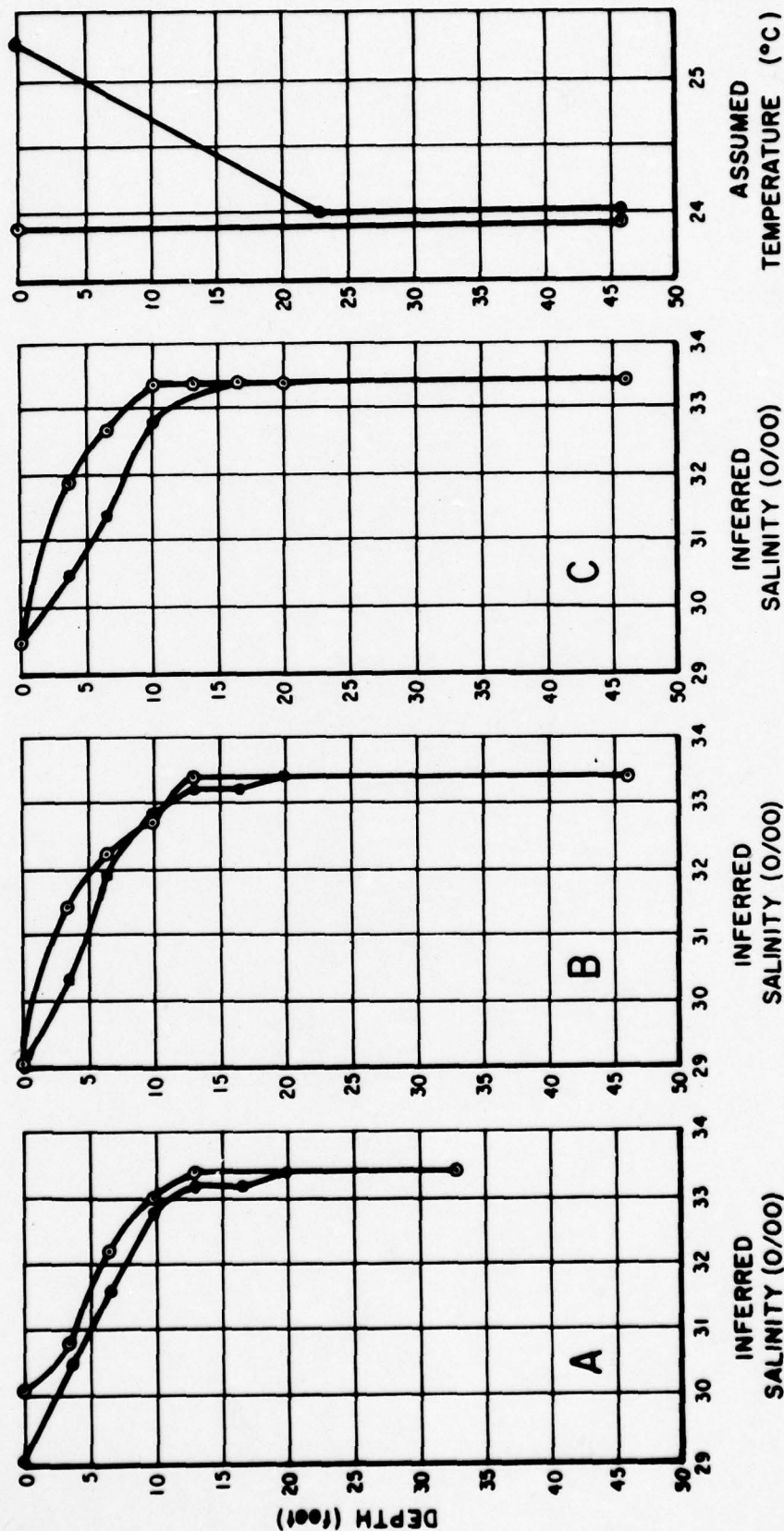
○——○ 8 MARCH VELOCITY PROFILE, ISOTHERMAL ASSUMPTION
●——● 13 MARCH VELOCITY PROFILE, TEMP. PROFILE #2

where,

d_L = depth of positive gradient

d_s = source depth

C_v = velocity of sound in isovelocity region (below the gradient)

ϕ_L = angle of a ray at a distance from the source

ϕ_s = angle of a ray at the source

For the limiting ray ($\phi_L = 0$):

$$\cos \phi_s = 1 - \frac{(d_L - d_s)\, g}{C_v}$$

The range at which this ray reaches the top of the isovelocity layer is:

$$R_h = \frac{C_v}{g}\, \sin \phi_s$$

If the positive gradient water column thickness, d_L, is 10':

$\phi_s = 2° 34'$

$R_h = 224'$

If $d_L = 20'$:

$\phi_s = 3° 37'$

$R_h = 316'$

Rays leaving the source at angles $-\phi_s < \phi < \phi_s$ are RSR* rays.
Rays leaving the source at angles such that $|\phi| > |\phi_s|$ are SRBR* rays.

———————————

* RSR: Refracted, surface reflected

SRBR: Surface reflected, bottom reflected

The RSR rays tend to generate shadow zones throughout the surface duct. These zones will be filled in with contributions from SRBR rays so that significant amounts of energy will exist throughout the duct. However, hot spots will exist throughout the surface duct wherever caustics occur. The existence of this surface duct would significantly complicate the calibration of sonar source level or sensitivity, but would not affect range or bearing calibrations.

An additional complication that would enter into the calculations would be handling the surface image (Lloyd mirror effect) under conditions that are non-isovelocity, but this could be done with a ray tracing program.

These considerations lead to the following general conclusions:

(1) The positive gradient layer is so shallow that a source or receiver probably would not be placed in it except for the case of calibrating a hull-mounted surface ship sonar.

(2) For a 10' layer the limiting rays occur at grazing angles of $\pm$ 2° 34' and the corresponding distance to the beginning of the first shadow zone is 224 ft.

(3) For a 20' layer the limiting rays occur at grazing angles of $\pm$ 3° 37' and the first shadow zone begins at 316 ft.

(4) The shadow zones would probably be filled in with energy from SRBR rays at the ranges of interest to SACS.

(5) For a first approximation, the assumption of straight line propagation and spherical divergence is adequate over the ranges of interest (hundreds of feet).

B. BOTTOM REFLECTION LOSS

1. Description of Procedures

Acoustic bottom loss measurements, at several grazing angles including 90°, were made at five locations in the test Slip (see Figure 7). The measurement platform was a painter's camel which was attached to a line passing down the centerline of the Slip. At each measurement location the camel was tied to the line and the position was determined by noting a prominent object on the shore line. The distance between the object and the nearest surveyor's mark on the curbing around the Slip was measured so the positions could be located on a chart of the slip. The vertical incidence measurements were made by suspending a projector and hydrophone from the northeast end of the camel. The approximate depths used were 35 feet for the projector and 43 feet for the hydrophone. The projector used was an element from a UQC transducer and the hydrophone was a USRL standard CH-1A made by Clevite. We tried using a USRL J-9 projector but the source level was too low. With the exception of the hydrophone battery box, the
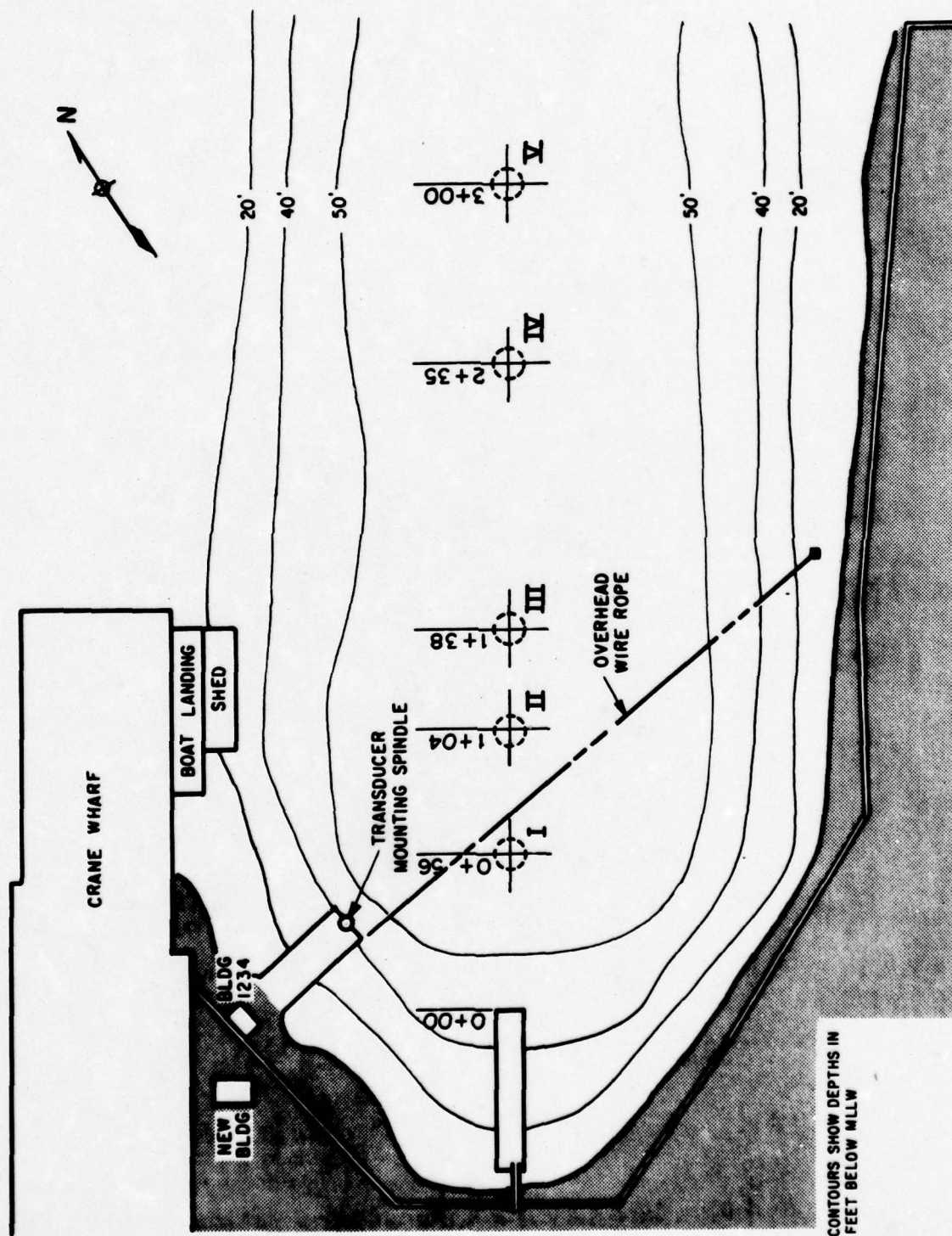
WET TEST SLIP
ACOUSTIC DATA STATIONS
FIGURE 7

CONTOURS SHOW DEPTHS IN
FEET BELOW MLLW

electronic equipment was located in a van onshore. The battery box supplied power to the hydrophone preamplifier and had to be placed on the camel because of the short cable supplied with the hydrophone. The hydrophone output and projector input were each cabled to the van by means of 250 feet of coaxial cable. An oscillator and an oscilloscope, both battery operated, were used on the camel to insert calibration signals into the receiving system. The magnitude of these signals was measured in the van and the gain of the system computed. The receiving equipment in the van is shown schematically in Figure 8.

FROM HYDROPHONE → AMPLIFIER → TAPE RECORDER / FILTER → SCOPE
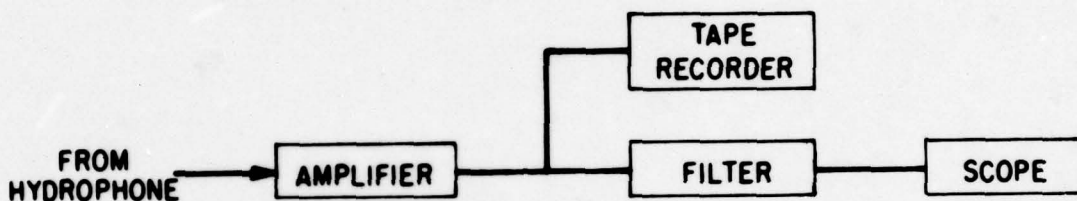
RECEIVING EQUIPMENT LOCATED IN VAN
FIGURE 8

In addition to recording on tape, recordings of the sound pulses were made from the oscilloscope using a polaroid camera. (Typical records are shown in Figures 9 and 10.) The transmitting electronics, also located in the van are shown schematically in Figure 11.

OSCILLATOR → TONE BURST GENERATOR → AMPLIFIER → TUNING REACTOR → TO PROJECTOR
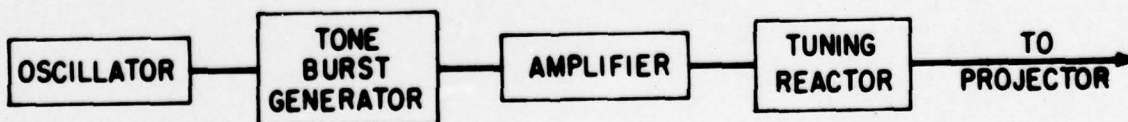
TRANSMITTING EQUIPMENT IN VAN
FIGURE 11

The measurements were made at frequencies of 3.5, 5 and 10 kHz with pulse lengths of approximately 2 msecs.
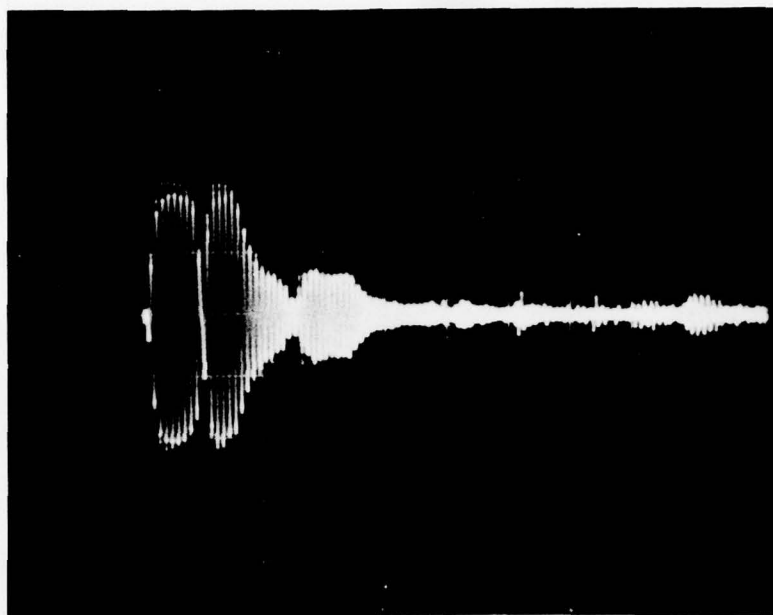
TYPE: P   POSITION: Ⅴ

FREQUENCY: 5kHz   DEPTH: 35 & 40 FT.
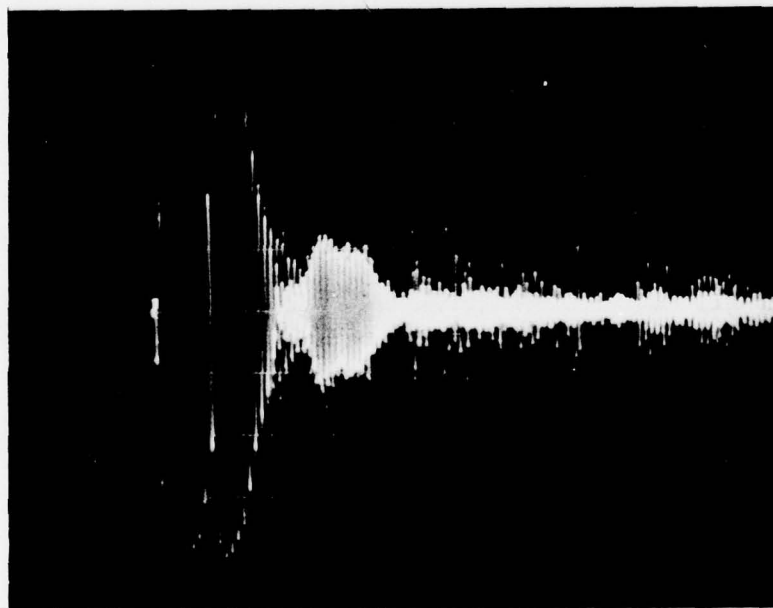
TYPE: P   POSITION: Ⅴ

FREQUENCY: 5kHz   DEPTH: 35 & 40 FT.

TYPICAL RECORDS
NORMAL INCIDENCE
FIGURE 9
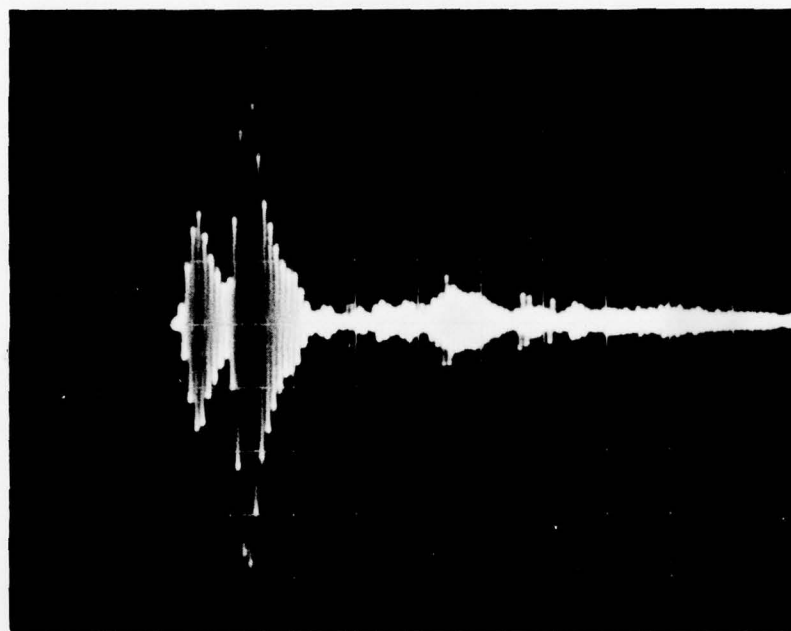
-16-

TYPE: S   POSITION: V
FREQUENCY: 5kHz   DEPTH: 35 FT.
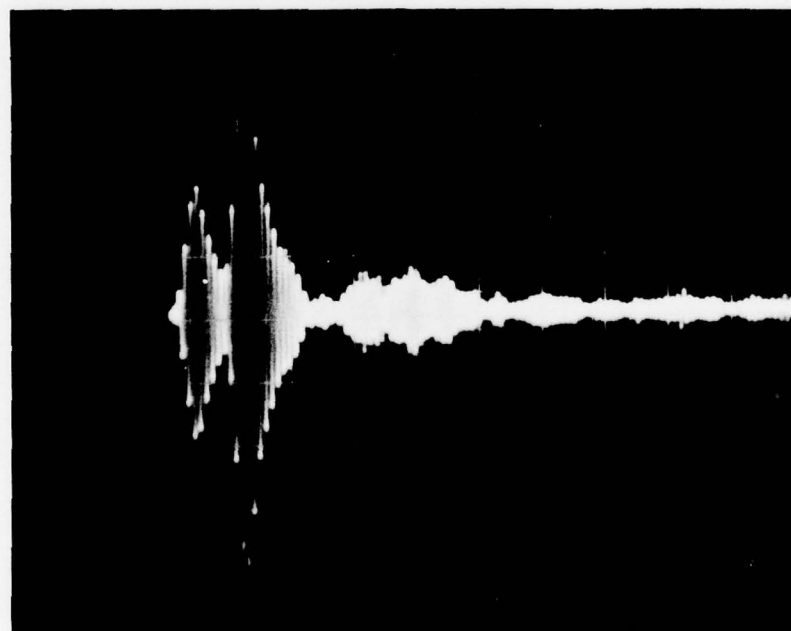
TYPE: S   POSITION: V
FREQUENCY: 5kHz   DEPTH: 40 FT.

TYPICAL RECORDS
OFF-NORMAL INCIDENCE
FIGURE 10

-17-

The bottom loss measurements at grazing angles other than 90° were made with the same projector and hydrophone with the addition of one more CH-1A hydrophone. The projector and hydrophones were mounted on a pipe frame as shown in Figure 12.
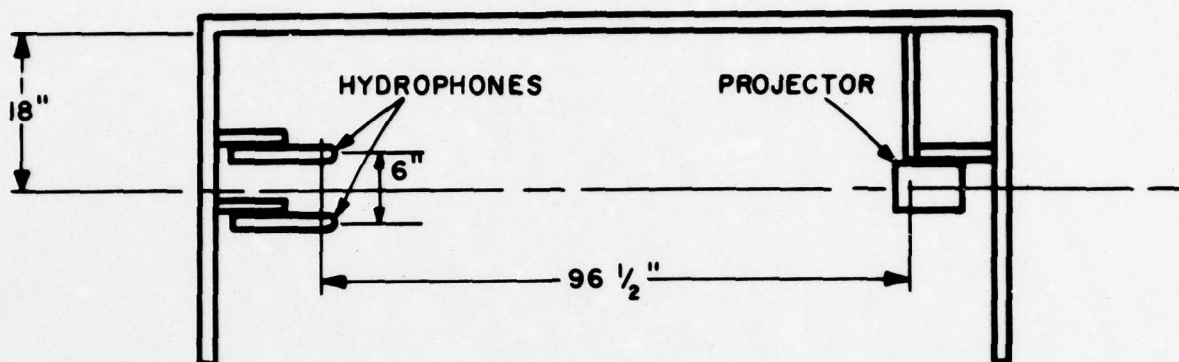
PIPE FRAME SUPPORTING
PROJECTOR AND HYDROPHONE
FIGURE 12

The pipe frame was supported by means of a rope bridle and depth settings were determined from tape markings on the cables. The transmitting electronics were the same as for the normal incidence measurements and the measurements were made at 5 and 10 kHz. Both hydrophones were amplified and recorded broadband (i.e., no filtering) on magnetic tape. In addition, the top hydrophone output was filtered after amplification, placed on the scope and recorded with a polaroid camera.

It can be seen from Figure 12 that the hydrophones would receive the direct arrival along the mechanical rather than the acoustic axis. Because of concern about the response of the hydrophones in this direction, we discussed the problem with Mr. W. Paine of the Underwater Sound Reference Division of the Naval Research Laboratory. He supplied us with vertical beam patterns at 3.5, 5.0, 6.4, 8.0, 10.0, 12.0 and 14.0 kHz for the CH-1A hydrophones, which are reproduced in the Appendix. Since the variation in these patterns at the angles of interest is only about 1 db, we did not make a correction.

The off-normal incidence measurements were made at three stations in the test slip; I, III, and V (see Figure 7). Two hydrophones were used and their outputs recorded separately because they will be treated as a dipole when the tape is played out. A dipole response is obtained by subtracting the two hydrophone channels when they are played out. The mounting of the hydrophones is such that the null in the dipole pattern is directed toward the projector. At the smaller grazing angles, the arrival times of

the direct and reflected pulses will be almost the same. The dipole is used to suppress the direct arrival so that a good measurement of the reflected pulse can be made. By having the two hydrophones recorded separately we can also obtain the magnitude of the direct pulse by looking at just one channel or by adding the channels (when the direct and reflected arrivals can be resolved).

2. Results

Bottom loss data that was photographically recorded has been reduced and analyzed. The data recorded on magnetic tape has yet to be reduced because of difficulties in obtaining suitable tape playback equipment.

The results obtained so far are presented in Figures 13 and 14. Figure 13 shows the bottom losses observed at Stations I, III, and V, which are the only locations at which measurements were made both at normal incidence and at various grazing angles. These are plotted against grazing angle for two frequencies, 5 and 10 kHz. Figure 14 shows the results obtained at all locations without differentiating the frequencies and grazing angles. (These points include data taken at 3.5, 5 and 10 kHz.)

The most striking characteristic of the data obtained is its variability. This is further illustrated by the comparison of means and standard deviations given in Table I.

The data of stations I and V show an apparent dependence of bottom loss upon grazing angle. This was not observed at Station III; nor do published results lead one to expect such a strong dependence. For the range of grazing angles observed, the bottom loss for this location would be about 20 db with only a slight decrease as the angle approaches normal incidence, according to results obtained by the Naval Electronics Laboratory*. For all the data analyzed, the apparent bottom loss varies from a high of about 16 db at Station I to a low of about -6 db at Station IV (i.e., a gain of 6 db). Correlations with frequency, grazing angle, and position are either non-existent or inconsistent with the physical situation (as established in part by known facts and in part by assumptions). In view of these results, it is necessary to seek an explanation by one of two avenues. Either the experimental methods were faulty or there are mechanisms at work (which were not anticipated) to account for the extreme variability in the results.

We have carefully reviewed the equipment and the techniques utilized to obtain the data. We have also reviewed the order in which individual observations were made to determine if results obtained with repeated set-ups at the same station were repeatable. Neither offers evidence to establish that the equipment or techniques were at fault.

---

* Information provided by Lyle C. Fisher in a letter to Arthur D. Little, Inc., dated 30 November 1965.
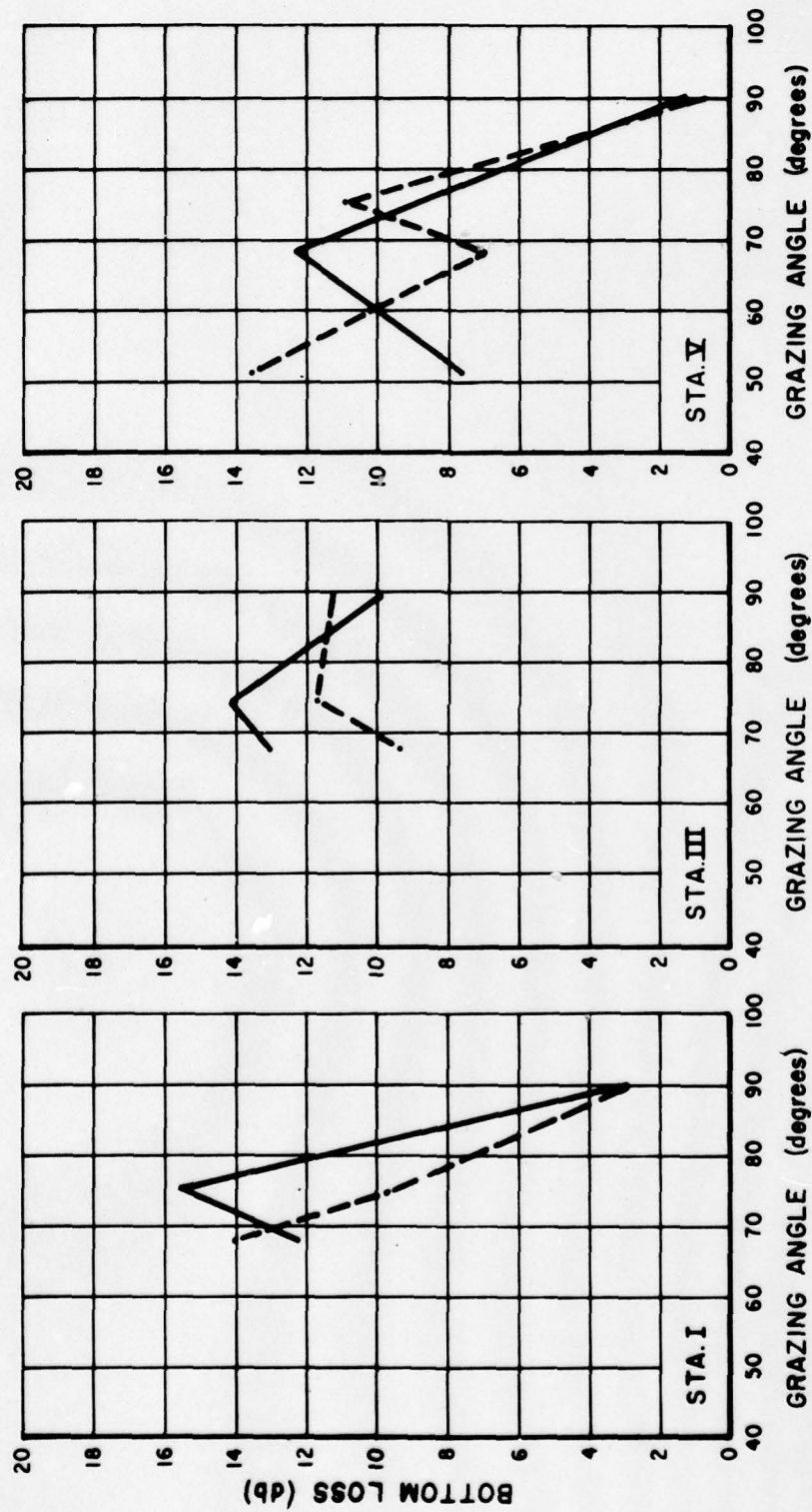
BOTTOM LOSS VS.
GRAZING ANGLE
FIGURE 13

BOTTOM LOSS (db)

NORMAL INCIDENCE DATA
OFF – NORMAL DATA
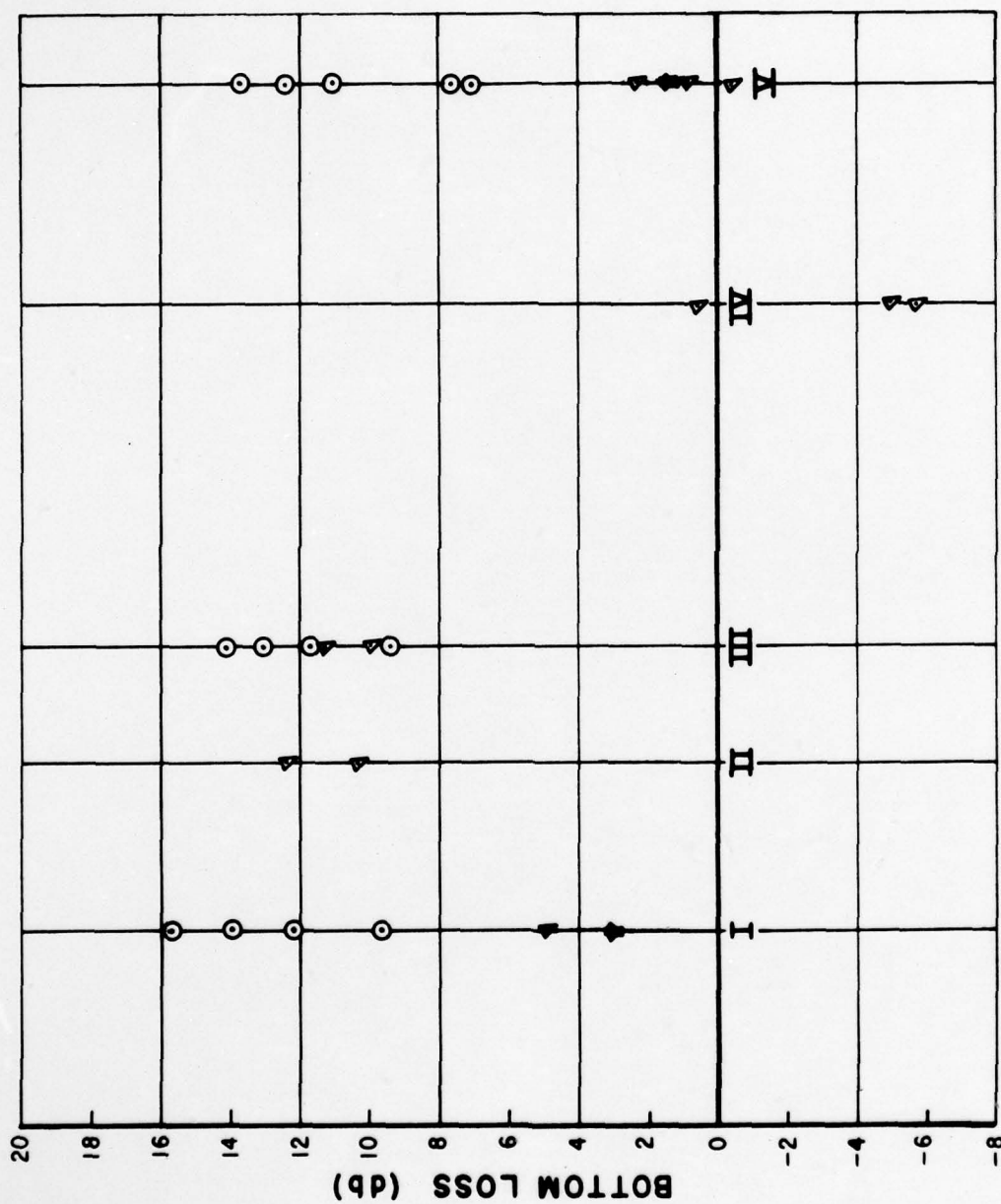
BOTTOM LOSS DATA
FIGURE 14

-21-

TABLE I

MEAN AND STANDARD DEVIATIONS

FOR BOTTOM LOSS DATA

Station	Mean Bottom Loss (db)	Standard Deviation (db)
I	8.9	5.4
II	11.4	*
III	11.6	1.8
IV	0.03	*
V	5.7	5.3
Pooled data (IV eliminated)	8.5	5.0

*Sample too small to compute
standard deviation.

We have investigated two mechanisms which could well account for the variability observed. One is divergence of the refelcted signal due to small curvatures in the bottom contours. The other is the addition (interference) of signals received from multiple layers below the first bottom. Divergence could account for a variation of from 5 to 10 db or more in the results, and echoes received from reflecting layers could account for 5 to 15 db in the variation. Discussions and analyses of these two mechanisms are contained in the Appendix.

3. Conclusions

It is possible--in fact, it seems likely--that the actual bottom loss in the Wet Test Slip is considerably higher than the simple average of these results.

The potential importance of effects such as those of divergence and interference from a layered bottom may lead to a conclusion of greater significance. That is, the general method of approach used here to obtain the acoustic characteristics of a relatively shallow and limited basin may lead to erroneous results. Basically, the approach used was to make a series of measurements, point by point, with the intention of combining these results in such a way as to characterize the acoustic properties of the basin as a whole.

It appears that much more detailed information; much more precise location of experimental equipment; and many more observation points should be utilized for this approach to yield valid results. For example, the bottom contours must be known in detail and the test equipment must be positioned at a precisely known point if the effects of divergence are to be properly accounted for. This would require a great deal more surveying than was possible within the constraints of this operation.

An alternative approach might utilize entirely different equipment and techniques. One might use an experimental source of much higher power and measure the acoustic signals received at many points for various locations of the source. Then the signals received would be the result of many effects combined, i.e., direct transmission, reflections, divergence, reverberation, multiple-bottoms, and so on. It probably would not be possible to separate these effects, but if sufficient observations were made, the location could be suitably described in terms of its gross acoustic characteristics as a location for a particular class of calibration measurements.

C. BOTTOM LAYERS

At our request, arrangements were made by NAVOCEANO to have bottom cores taken in the Test Slip. A piston coring tool was used to obtain cores approximately five feet long in three locations (shown in Figure 15). The tool was positioned and lowered by yard crane P-59. The tool was loaded with 150 pounds and fell approximately 15 feet through the water before impacting the bottom.

Arthur D. Little, Inc.

N

CRANE WHARF

BOAT LANDING
SHED

BLDG
1234

NEW
BLDG

NO. 1

NO. 2

NO. 3

TRANSDUCER
MOUNTING SPINDLE

BORING #73

OVERHEAD
WIRE ROPE

BORING
#68

BORING #63

20' 40' 50'

50' 40' 20'

CONTOURS SHOW DEPTHS IN
FEET BELOW MLLW
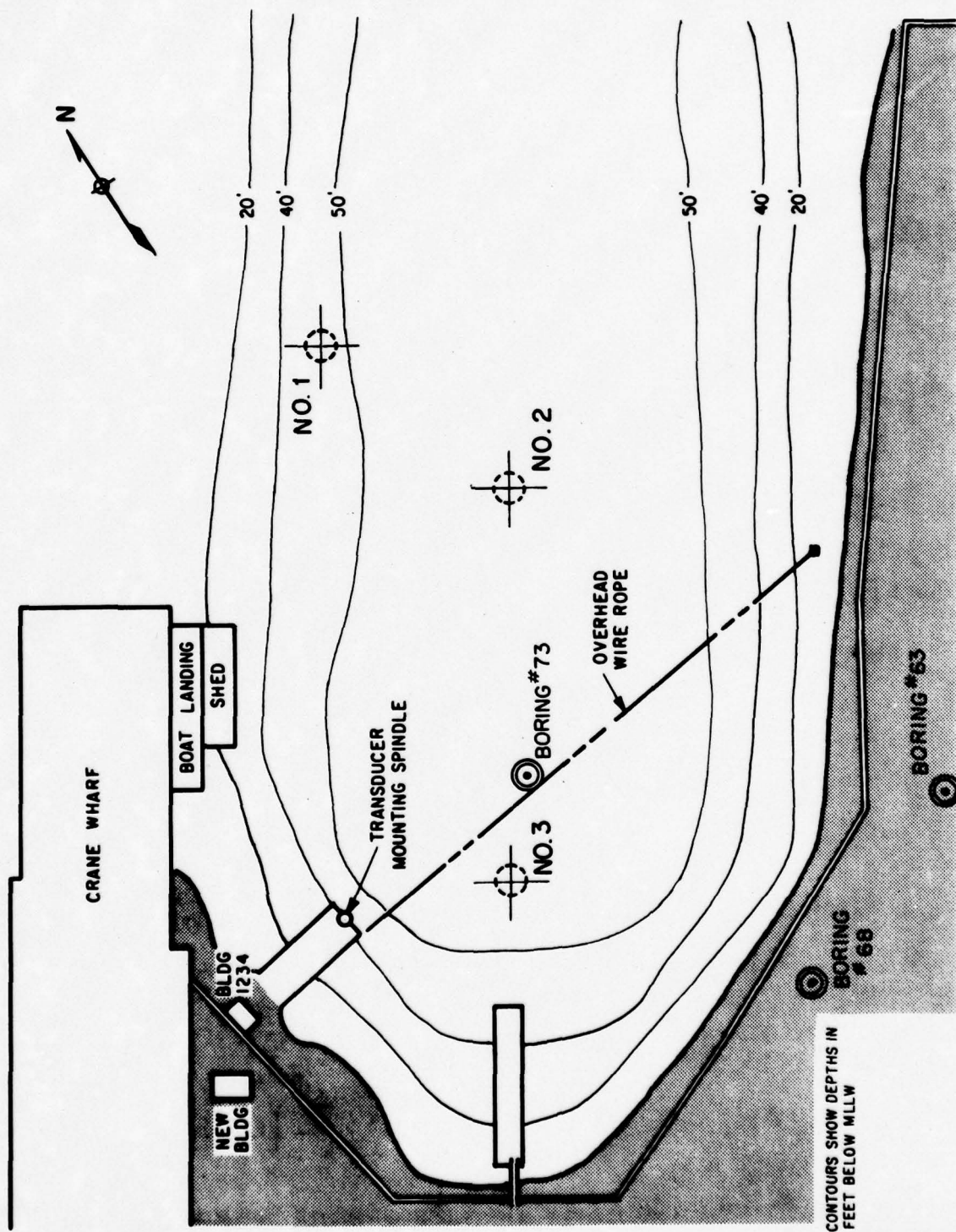
WET TEST SLIP
BOTTOM CORE AND BORING LOCATIONS
FIGURE 15

-24-

Unfortunately, the penetration attained was not sufficient to provide information about layering below the bottom. However, porosity, which is a parameter of primary importance in determining the reflection loss analytically, was obtained. Analysis of the cores was performed by NAVOCEANO. For completeness, their report on the cores is included, in its entirety, in the Appendix.

The NAVOCEANO report was reviewed and an attempt made to relate its content to earlier estimates of the bottom and its effect on reflection coefficient.

Prior to receiving this NAVOCEANO document we assumed that the conditions were a water column of 51.5 feet overlaying a clay bottom extending 8.4 feet and then a layer of hard limestone and coral. We further assumed that the clay bottom had a density of 1.5 grams/cm^2 and the limestone a density of 2.5 grams/cm^2.

The core analysis substantiates this in part but unfortunately, the deepest core obtained was approximately 6.5 feet; thus, the second layer, if existing, was never reached.

Core #1 yielded no information but cores #2 and #3 did. The wet unit weight (the weight of solids plus water per unit volume of the sediment mass) is closely related to the in situ density and, for cores #2 and #3, it had a mean value of 1.547 grams/cm^3 with a standard deviation of 0.045. This is very close to the assumed density (1.5). Since the density and porosity are linearly related (to a first approximation) one would expect the porosity to be relatively constant. This proved to be true for cores #2 and #3 where the measured porosity had a mean of 66.82% with a sigma of 2.3.

Throughout the cores the percentage of calcium carbonate varied from 91.8% to 0 with percentages between 30% and 50% being common. This would be expected in light of the coral and shells in that general area.

One very interesting result was the lack of any trace of organic carbon which would make one suspect that the sewage being dumped into the Wet Slip is probably being washed out of the Slip rather than precipitating to the bottom.

Figure 16 shows the per cent of sample by weight present in cores #2 and #3 for gravel, sand, silt, and clay. The porosity is also indicated. While varying somewhat over the length of the cores, there are no gross changes that would indicate a significant change in acoustic properties. This is in line with our previous assumption of an 8.4 foot layer of clay.

The acoustic data revealed echoes which appear to come from layers below the bottom. The water depth from the acoustic data is about 50 feet. Echoes were received quite consistently from a stratum whose apparent depth was about 54 feet. (True depth could not be computed because the sound velocity could not be measured in the cores obtained.)

-25-

PERCENT OF SAMPLE (by weight)
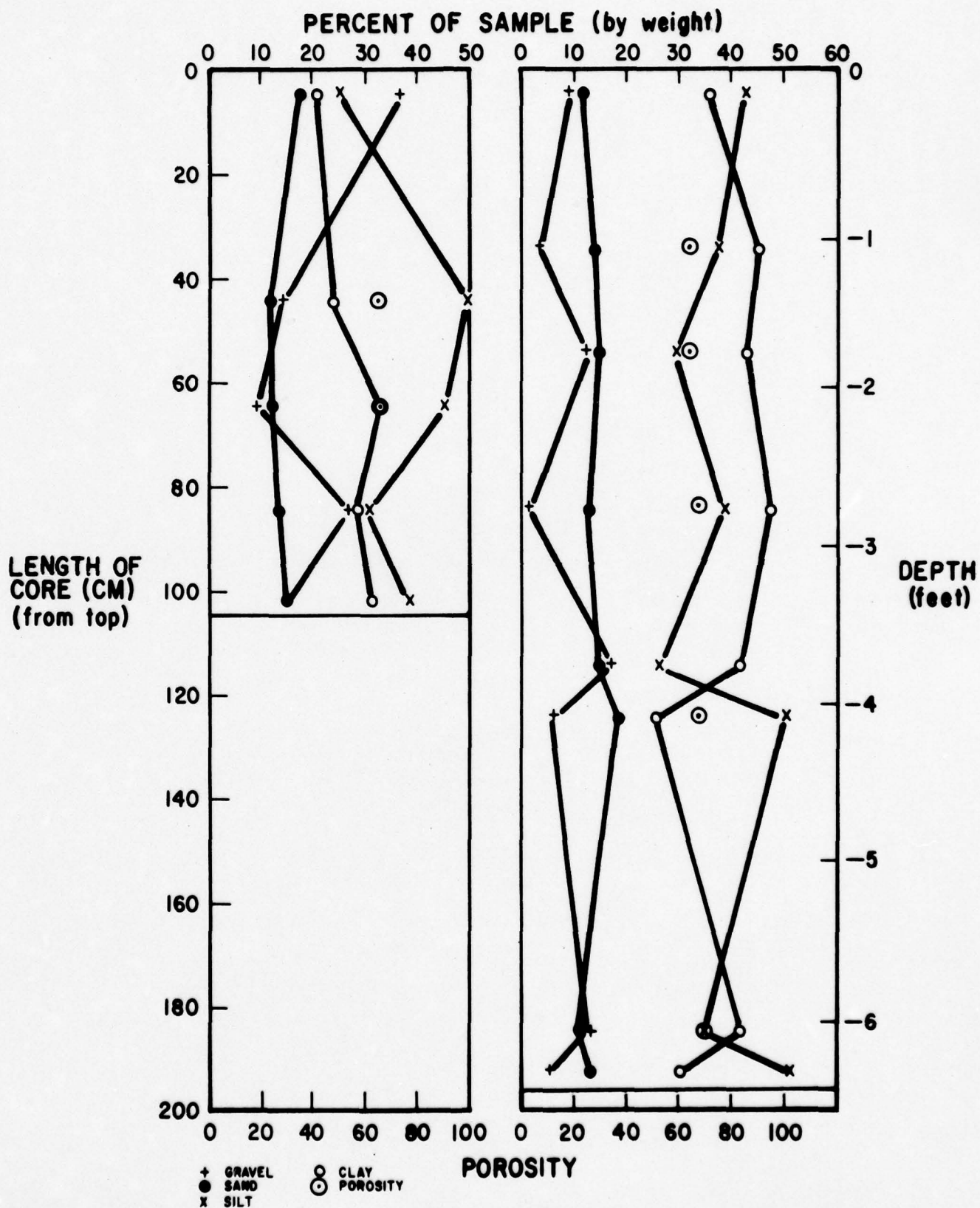
ANALYSIS OF CORE

FIGURE 16

-26-

With less consistency, echoes were also received from a second and even a third layer below the bottom. The presence of these returns lends credence to the hypothesis that some of the variability experienced can be accounted for by the interference of multiple echoes from sub-bottoms.

Additional evidence of bottom layers is shown in boring data which was obtained from the public works office of the shipyard. Locations of the bore holes (which were made in 1940) are shown in Figure 15, and the data is reproduced in Tables II, III, and IV.

D. AMBIENT NOISE

While making tests in Pearl Harbor it was noticed that the ambient noise was of a somewhat different character than normally encountered. The noise, when viewed broadband on an oscilloscope, appeared to be very spikey. It appeared as though discrete noise sources were randomly generating very narrow noise pulses. At first this was attributed to electrical noise in the shipyard. However, as the noise appeared to be acoustic in origin it was decided that the source might very well be snapping shrimp.

A crude test was run to obtain an "order of magntidue" estimate of the noise level. Measurements were made using a standard hydrophone, preamplifier, two filters, and a VTVM. The VTVM was not a true r.m.s. meter as one was not available.

The hydrophone was located approximately at Station I, Figure 7. Measurements were made at a depth of 25 feet.

Figure 17 shows the filter bandwidth used for the measurements. A −3 db bandwidth of 2.86 kHz was used for the calculations.

The ambient noise generated a voltage between 5 and 7 millivolts on the VTVM. At the filter center frequency the system gain was found to be a factor of 28. Using a hydrophone sensitivity of −89 dbv/μbar, a system gain of 28 (29 db), a bandwidth of 2.86 kHz, and a noise output voltage of 6 millivolts, the noise level may be obtained as follows:

$$E_{in} = E_{out} - \text{Gain} = -44.4 \text{ dbv} - 29 = -73.4 \text{ dbv}$$

$$N_p = -73.4 \text{ dbv} - (-89 \text{ dbv/μbar}) = +15.6 \text{ db re 1μbar}$$

In a 1 Hertz bandwidth:

$$SPL = N_p - 10 \log Bw = 15.6 - 34.5 = -18.9 \text{ db re 1μbar/Hertz}$$

This number is within 10 db of levels reported in earlier studies. These studies indicated that snapping shrimp noise was intense and became more intense as the water depth decreased. Since the current tests were run in considerably shallower water than the earlier tests, it is not surprising that the new data indicated 10 db more ambient noise

Arthur D. Little, Inc.
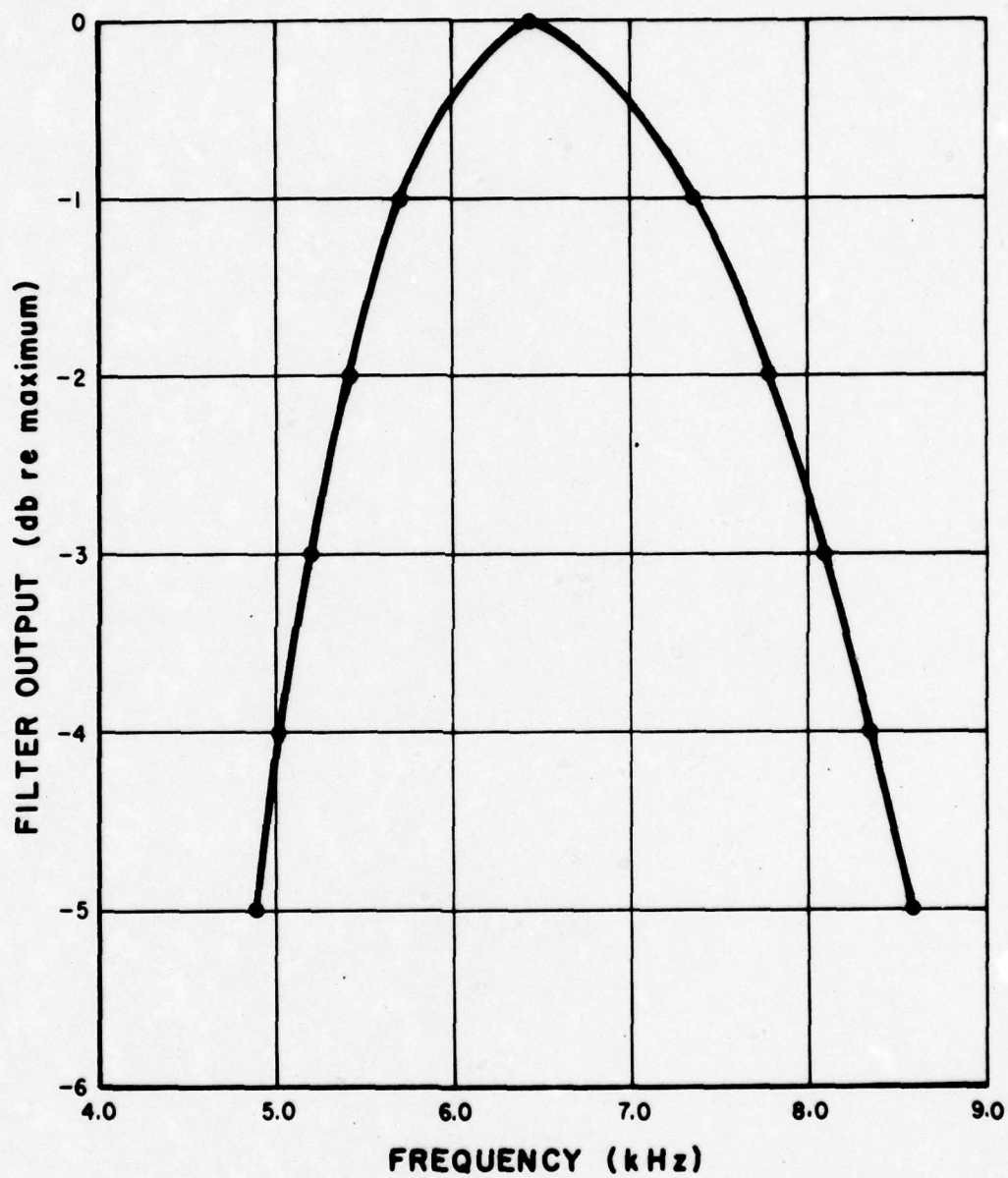
SYSTEM BANDWIDTH
FOR NOISE MEASUREMENTS
FIGURE 17

108.1	
105.6	Loose sand and coral fragments
102.0	Limestone, silty, loose and soft
M.L.W.	- -
	Volcanic tuff, hard, to limestone, fine, sandy, weakly cemented
95.4	
91.7	Limestone, hard reef coral
	Limestone, coarse, sandy, strongly cemented
83.6	
	Limestone, coarse, sandy, strongly cemented and fragments
73.6	
72.0	Limestone, hard reef coral
	Limestone, hard reef coral fragments
63.6	
	Honeycombed hard reef coral with pockets of loose coral fragments, sand and silt
53.6	
	Clay, compact, brown
47.1	
	Limestone, hard reef coral and fragments
40.1	
	Limestone, silty, loose and soft, containing coral fragments, with occasional thin strata of hard reef coral
27.4	
	No sample recovered
21.2	
	Coarse, loose, limestone sand and hard reef coral fragments
14.6	

TABLE II

BORING NO. 73

-29-

Depth		Description
112.0		
109.5		Coral fill
107.5		Limestone, coarse, sandy, strongly cemented
107.0		Adobe
		Volcanic tuff, medium hard and soft, with some volcanic
102.0		sand, strongly consolidated
M.L.W.		
97.0		Clay, soft, brown
93.5		Clay, soft, brown, containing coral fragments
		Limestone, coarse, sandy, strongly cemented, with occasional pockets of loose fragments
82.1		
77.0		Limestone, silty, strongly cemented fragments and limestone, silty, loose and soft
72.0		Limestone, fine, sandy, loose and soft
		Honeycombed hard reef coral with pockets of loose coral fragments, sand and silt
62.0		
59.0		Limestone, hard reef coral and fragments
57.0		Mixture, brown clay and limestone, fine, sandy, loose and soft, containing coral fragments
52.0		Limestone, hard reef coral and fragments with pockets of coarse and fine coral sand
50.0		Limestone, fine, sandy, loose and soft
47.0		No sample recovered
		Limestone, hard reef coral and fragments with traces of limestone, silty, loose and soft
37.0		
		Honeycombed hard reef coral with pockets of loose coral fragments, sand and silt
23.0		
		Limestone, hard reef coral fragments and limestone, silty, strongly cemented fragments, with some limestone, fine sandy, loose and soft
14.9		

TABLE III

BORING NO. 68

-30-

Depth	Description
110.7	
108.2	Coral sand and coral fragments
104.4	Limestone, hard reef coral fragments
M.L.W.	Volcanic tuff, hard and soft
98.2	
	Limestone, hard reef coral and limestone, coarse, sandy, strongly cemented and fragments
86.0	
	Limestone, hard reef coral and fragments with trace of limestone, silty, loose and soft
80.0	
	Honeycombed hard reef coral with pockets of loose coral fragments, sand and silt
67.5	
	Limestone, hard reef coral fragments and limestone, fine, sandy and silty, loose and soft, containing coral fragments
60.0	
	Honeycombed hard reef coral with pockets of loose coral fragments, sand and silt
56.0	
	Clay, compact, brown
46.4	
	Limestone, hard reef coral and fragments
32.4	
	Fragments of limestone, hard reef coral and clay, soft, brown
26.6	
	Limestone, fine, sandy, loose and soft
21.1	
	Mixture, brown clay and limestone, fine sandy and silty, loose and soft
14.7	

TABLE IV

BORING NO. 63

APPENDIX

PART I

THE EFFECTS OF DIVERGENCE ON THE MEASUREMENT
OF BOTTOM REFLECTION COEFFICIENTS

I. INTRODUCTION

During the month of March, 1967, Arthur D. Little, Inc., partic
ipated in a measurements program in the Pearl Harbor Naval Shipyard. An
attempt was made to measure bottom reflection coefficients at a number of
stations in a Wet Slip. The reflection coefficients measured demonstrated
a large variability up to and including "gain" upon reflection.

This analysis attempts to explain the variability in terms of
divergence from a curved surface and indicates what order of magnitude of
curvature would be necessary to account for the station in which "gain"
was observed.

Using classical geometric optics, it is possible to explain the
anomolous behavior demonstrated by the reflection coefficient. When making
measurements of bottom reflectivity in very shallow water, or with a source
and receiver near the bottom, the effects of divergence after reflection
from a curved surface can easily over-ride the effect due to a lossy bottom.

Focusing, or divergence less than spherical, occurs if the bottom
is concave and becomes significant as the value of ρ, the radius of curva-
ture of the bottom surface, approaches d, the distance between the bottom
and the transducer.

Divergence greater than spherical occurs if the bottom is convex.
For small ratios of d/ρ, the effect is slight. However, as d becomes
larger than ρ, the effect becomes important.

The focusing effects demonstrated in the Pearl Harbor tests at
station IV, a gain of several db, could have been caused by reflections
from a concave surface as small as 5 feet in diameter with a radius of
curvature of 15 feet. This corresponds to a change in relief of 10 inches
in 5 feet.

The analysis indicates that the bottom contour must be known to
a high degree in cases where the distances between the transducer approxi-
mates the radius of curvature of the surface being insonified.

II. GENERAL ANALYSIS

This section leans heavily on the work of Riblet and Barker for
divergence from a curved surface[1]. A divergence anomaly is defined and

---

[1] N. J. Riblet and C. B. Barker, "A General Divergence Formula",
Journal of Applied Physics, Volume 19, p. 63, January 1948.

then its behavior is examined for the special cases of normal incidence reflection from spherical and cylindrical surfaces.

Riblet and Barker define the divergence as the ratio of the reflected energy per unit area to the incident energy per steradian. A general expression for divergence, D, is then derived in terms of the geometry shown in Figure A-1. The expression is:

$$D = \frac{\cos \Omega \; \rho_1 \; \rho_2}{F}$$

where:

$$F = \cos \Omega \left[4 \; d_1^2 \; d_2^2 + \rho_1 \; \rho_2 \; (d_2 + d_1)^2 \right]$$
$$+ \left[\rho_1 \; \sin^2 \theta_1 + \rho_2 \; \sin^2 \theta_2 \right] \; \left[2 \; d_1 \; d_2^2 + 2 \; d_1^2 \; d_2 \right]$$

and ρ_1 and ρ_2 are the principal radii of curvature of the surface.

The radius of curvature is obtained by finding the osculating circle that passes through the point of interest, and then taking the reciprocal of its curvature. If a curve is defined as:

$$y = f(x)$$

its radius of curvature is:

$$\rho = \frac{\left[1 + \left(\frac{dy}{dx} \right)^2 \right]^{3/2}}{\frac{d^2 y}{dx^2}}$$

The easiest cases to examine are those where the reflecting surface has the form of a cylinder or a sphere.

For a cylinder, letting $\rho_1 \rightarrow \infty$,

$$D = \frac{\rho_2 \cos \Omega}{\cos \Omega \; \rho_2 \; (d_1 + d_2)^2 + \sin^2 \theta_1 \; 2 \; d_1 d_2 \; (d_1 + d_2)}$$

if the incident energy is aligned with the X axis, then $\theta_1 = 0$, and

$$D = \frac{\rho_2 \cos \Omega}{\cos \Omega \; \rho_2 \; (d_1 + d_2)^2} = \frac{1}{(d_1 + d_2)^2}$$

or simple spherical divergence.
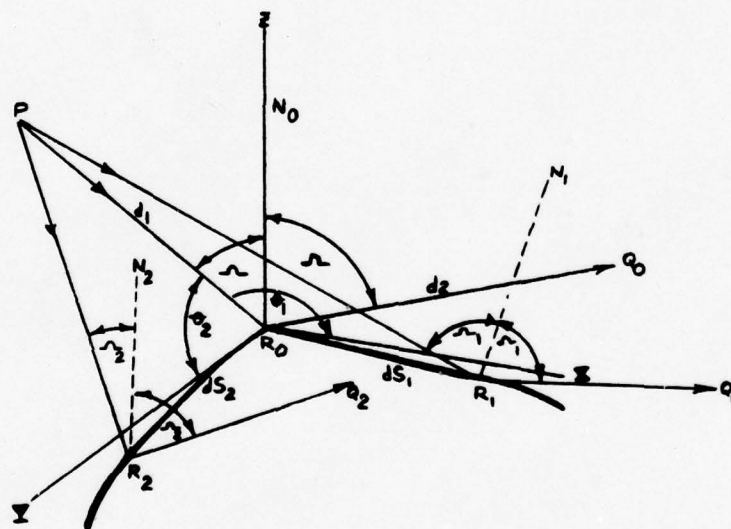
GEOMETRY AT
POINT OF REFLECTION

FIG. A-1

If the incident energy is aligned with the y axis, then $\theta_1 = 90°$, and

$$D = \frac{\rho_2 \cos \Omega}{\rho_2 \cos \Omega (d_1 + d_2)^2 + 2d_1 d_2 (d_1 + d_2)}$$

As $\rho_2 \to \infty$, D once again approaches spherical divergence.

For the case of normal incidence,

$$\Omega = 0 \text{ and } \theta = 90°, \text{ and}$$

$$D = \frac{\rho_2}{\rho_2 (d_1 + d_2)^2 + 2d_1 d_2 (d_1 + d_2)}$$

If $d_1 = d_2$, then, (for the cylindrical case),

$$D = \frac{\rho_2 \cos \Omega}{d^2 \rho_2 \cos \Omega + 4 d^3 \sin^2 \theta_1}$$

and

$$D_{\theta_1 = 0} = \frac{1}{d^2} ; \quad D_{\theta_1 = 90°} = \frac{\rho_2 \cos \Omega}{d^2 \rho_2 \cos \Omega + 4 d^3}$$

and

$$D_{\Omega = 0} = \frac{\rho_2}{d^2 \rho_2 + 4 d^3}$$

For a spherical reflecting surface, $\rho_1 = \rho_2 = \rho$, and

$$D = \frac{\rho^2 \cos \Omega}{\cos \Omega \left[4 d_1^2 d_2^2 + \rho^2 (d_1 + d_2)^2 \right] + \rho \left[(1 + \cos^2 \Omega) (2d_1 d_2) (d_1 + d_2) \right]}$$

For normal incidence, $\Omega = 0$, and

$$D_{\Omega = 0} = \frac{\rho^2}{4 d_1^2 d_2^2 + \rho^2 (d_1 + d_2)^2 + 4\rho d_1 d_2 (d_1 + d_2)}$$

If $d_1 = d_2 = d$

$$D_{\Omega = 0} = \frac{\rho^2}{4\ d^2\ (d + \rho)^2}$$

For a nonspherical surface, but still normal incidence, the result is very similar, namely,

$$D_{\Omega = 0} = \frac{\rho_1\ \rho_2}{4\ d^2\ (d + \rho_1)\ (d + \rho_2)}$$

Let us define a divergence anomaly as the divergence upon reflection from an arbitrary smooth surface divided by spherical divergence.

$$A_D = \frac{D}{1/(d_1 + d_2)^2}$$

This can be interpreted in terms of a loss or a gain as compared to reflection from a planar surface.

For the general case,

$$A_D = \frac{\rho_1\ \rho_2\ (d_1 + d_2)^2\ \cos \Omega}{\cos \Omega \left[4\ d_1^2 d_2^2 + \rho_1 \rho_2\ (d_2 + d_1)^2 \right] + \left[(\rho_1 \sin^2 \theta_1 + \rho_2\ \sin^2 \theta_2)\ (2 d_1 d_2^2 + 2 d_1^2 d_2) \right]}$$

For reflection from a cylindrical surface:

$$A_D = \frac{\rho_2\ \cos \Omega}{\rho_2\ \cos \Omega + \left[2\ d_1 d_2 / (d_1 + d_2) \right]\ \sin^2 \theta_1}$$

If $\theta_1 = 0$

$$A_D = 1$$

If $_1 = 90°$

$$A_D = \frac{\rho_2\ \cos \Omega}{\rho_2\ \cos \Omega + 2\ d_1\ d_2 / (d_1 + d_2)}$$

If $d_1 = d_2 = d$

$$A_D = \frac{\rho_2\ \cos \Omega}{\rho_2\ \cos \Omega + d\ \sin^2 \theta_1}$$

-38-

and, if $\Omega = 0$

$$A_D = \frac{\rho_2}{\rho_2 + d \sin^2 \theta_1}$$

and, if $\Omega = 0$ and $\theta = 90°$

$$A_D = \frac{\rho_2}{\rho_2 + d} = \frac{1}{1 + \frac{d}{\rho}}$$

For a reflection from a spherical surface:

$$A_D = \frac{\rho^2 (d_1 + d_2)^2 \cos \Omega}{\cos \Omega \left[4 d_1^2 d_2^2 + \rho^2 (d_2 + d_1)^2 \right] + \rho \left[(1 + \cos^2 \Omega) (2d_1 d_2) (d_1 + d_2) \right]}$$

At normal incidence:

$$A_{D \ \Omega = 0} = \frac{\rho^2 (d_1 + d_2)^2}{4 d_1^2 d_2^2 + \rho^2 (d_1 + d_2)^2 + 4\rho \ d_1 \ d_2 (d_1 + d_2)}$$

and if $d_1 = d_2 = d$

$$A_{D_{\Omega = 0}} = \frac{\rho^2}{(d + \rho)^2} = \left(\frac{1}{1 + \frac{d}{\rho}} \right)^2$$

Now, if $A_D < 1$ (or, expressed in db, less than zero) the divergence is greater than spherical. This occurs when $\rho < -2$ or, in all cases when the reflecting surface is convex.

Note that the anomaly for the sphere is the square of the anomaly for the cylinder in this simple case.

Figure A-2 shows the behavior of the divergence anomaly for the case $\Omega = 0$, and $d_1 = d_2$. The anomaly is approximately unity (or zero db) for a large radius of curvature or a small d, however, as $d \to \rho$ the anomaly gets large for a concave surface (gain). We may interpret values of $A_D > 0$db as a gain upon reflection and values of $A_D < 0$db as a loss upon reflection compared to what would be obtained upon reflection from a planar surface. For the purposes of this analysis it is assumed that the reflection coefficient is unity (no loss at the surface).

-39-

CONVEX

CONCAVE

A_0 (db)

d/p

DIVERGENCE ANOMALY
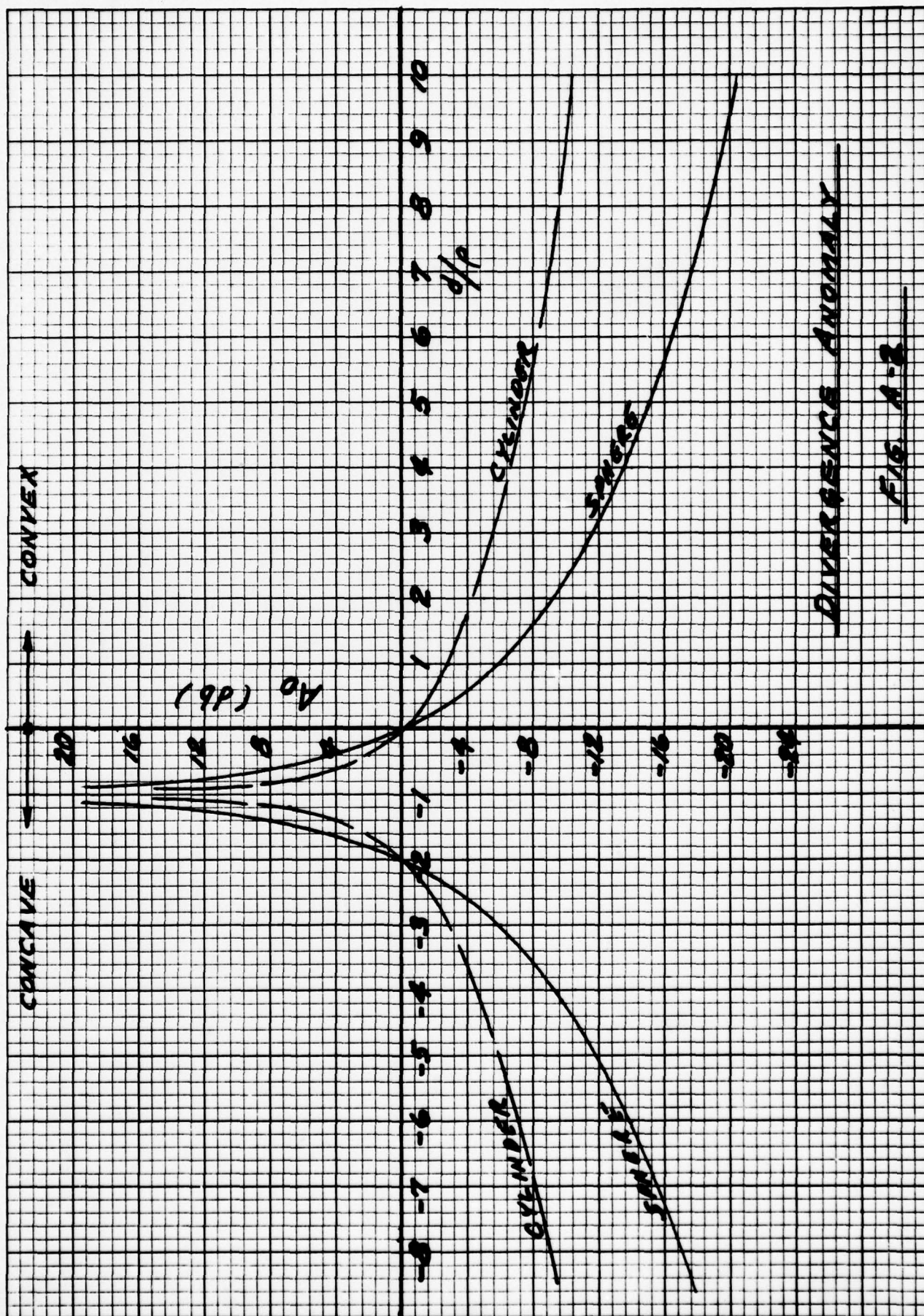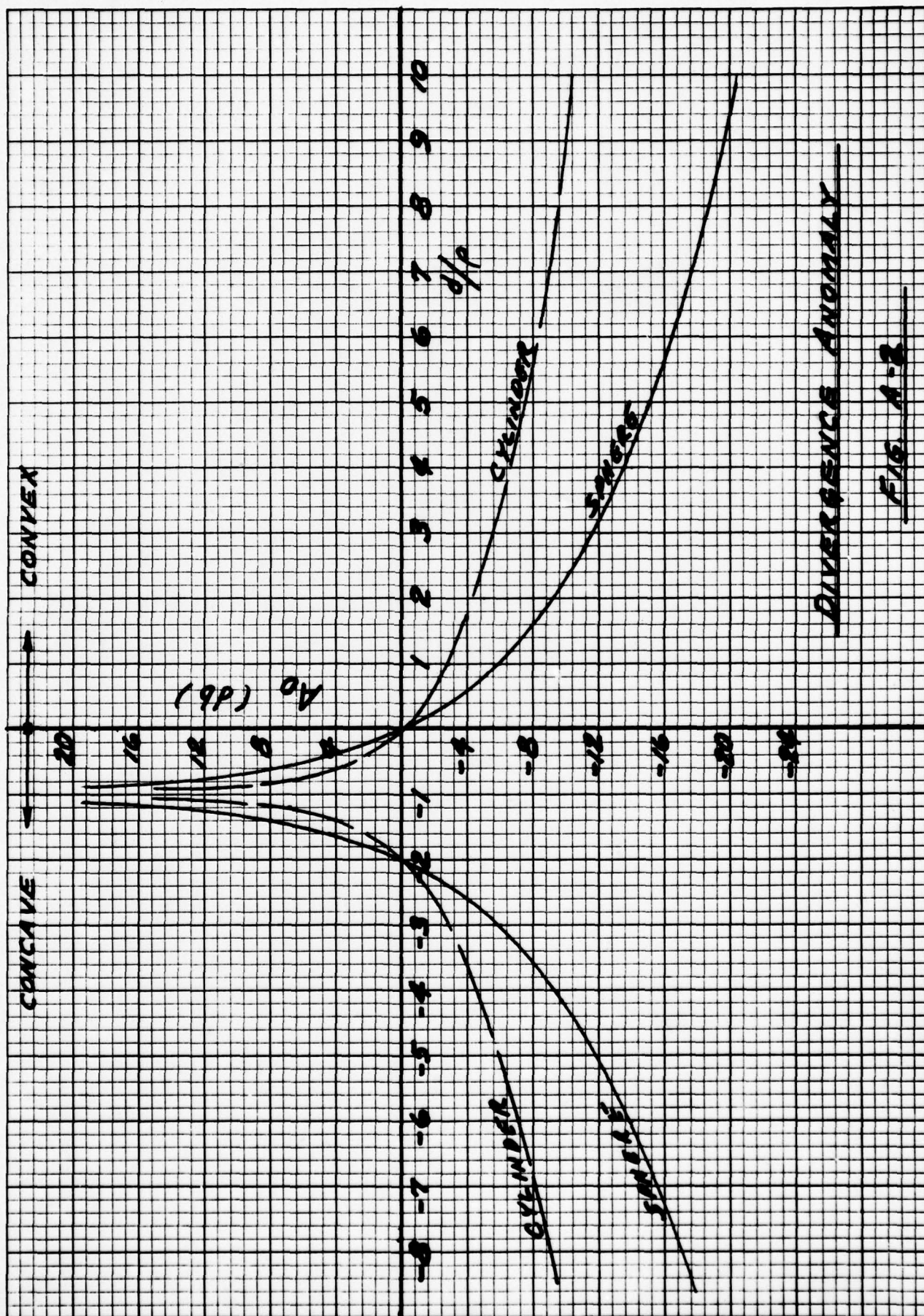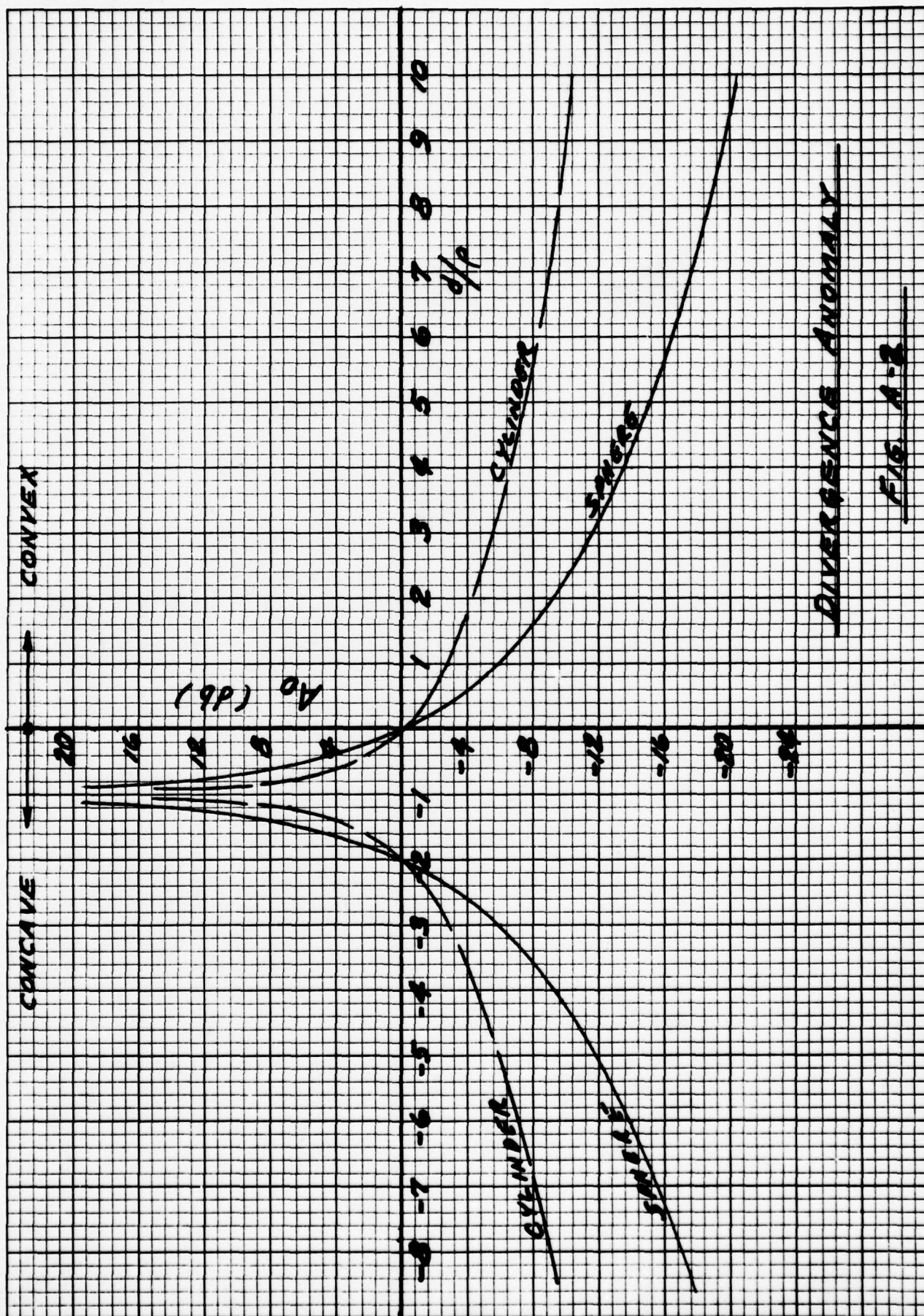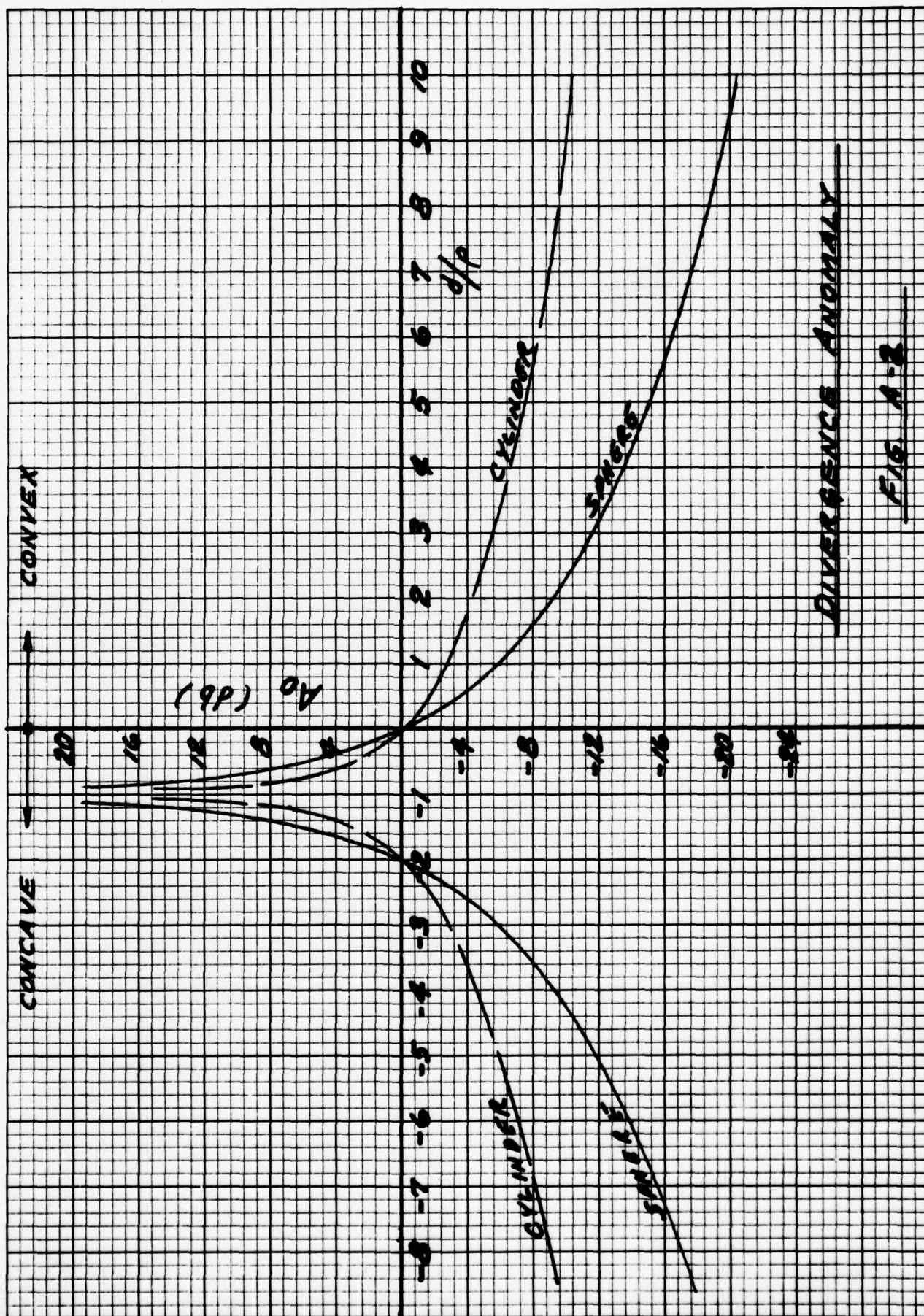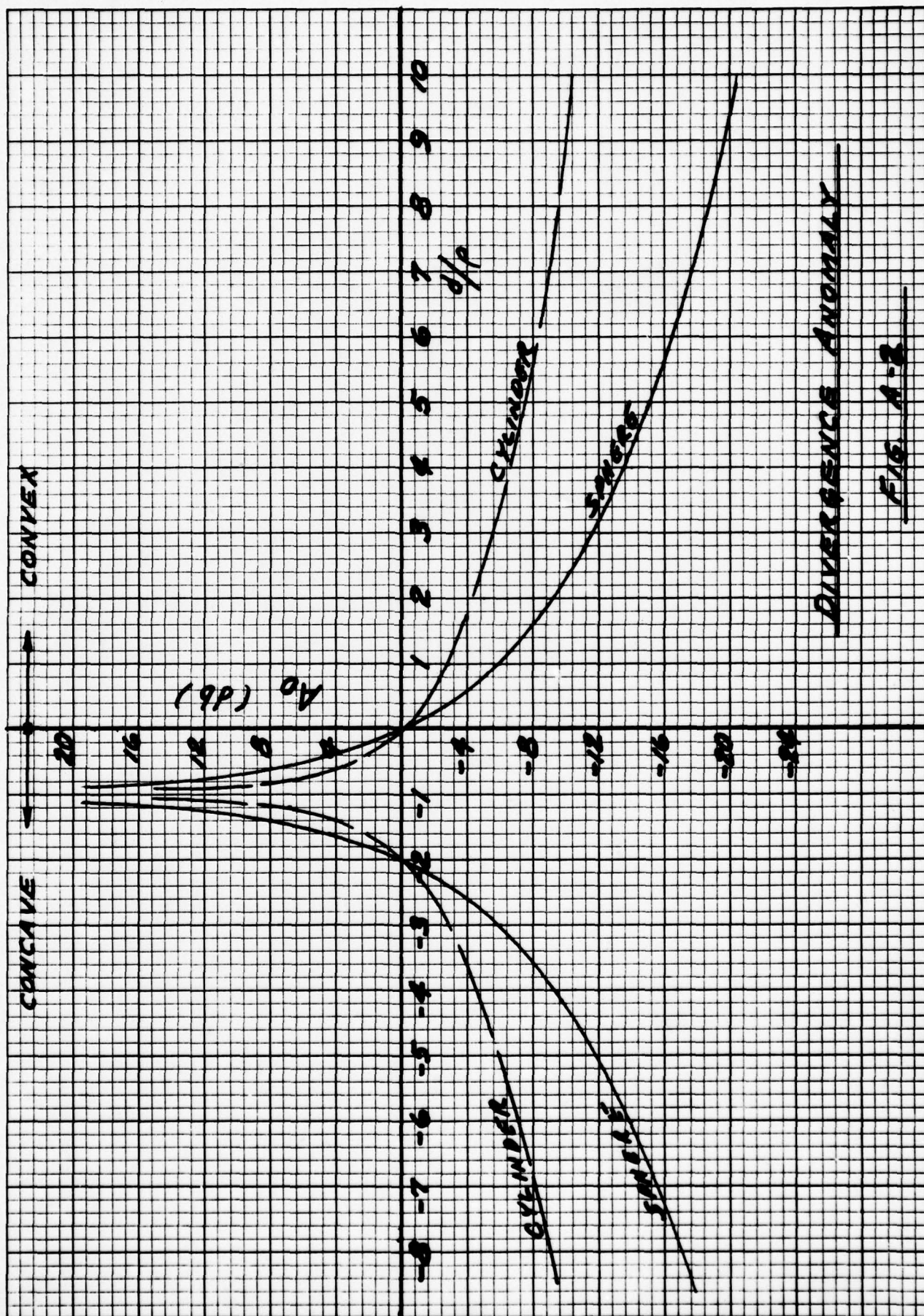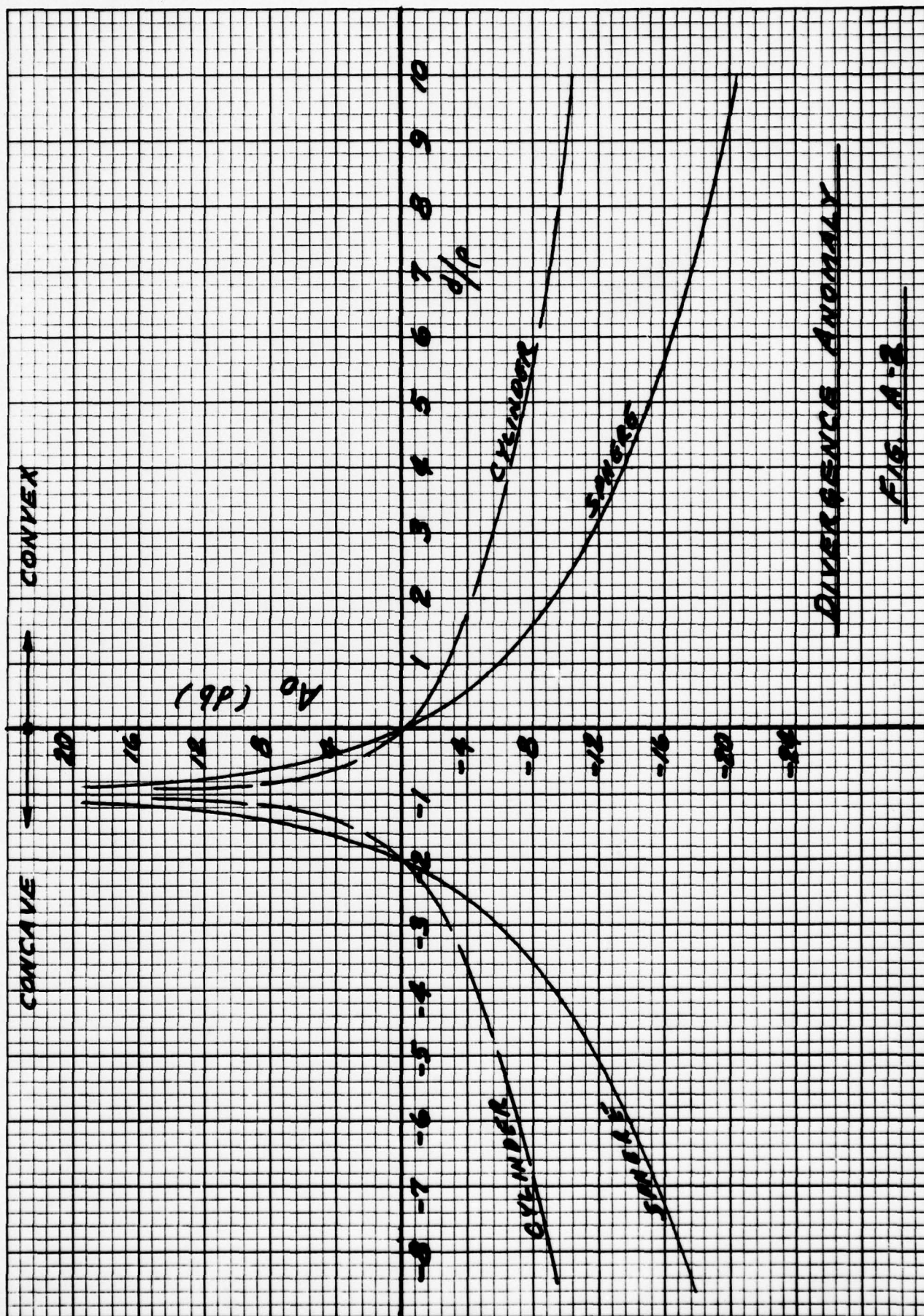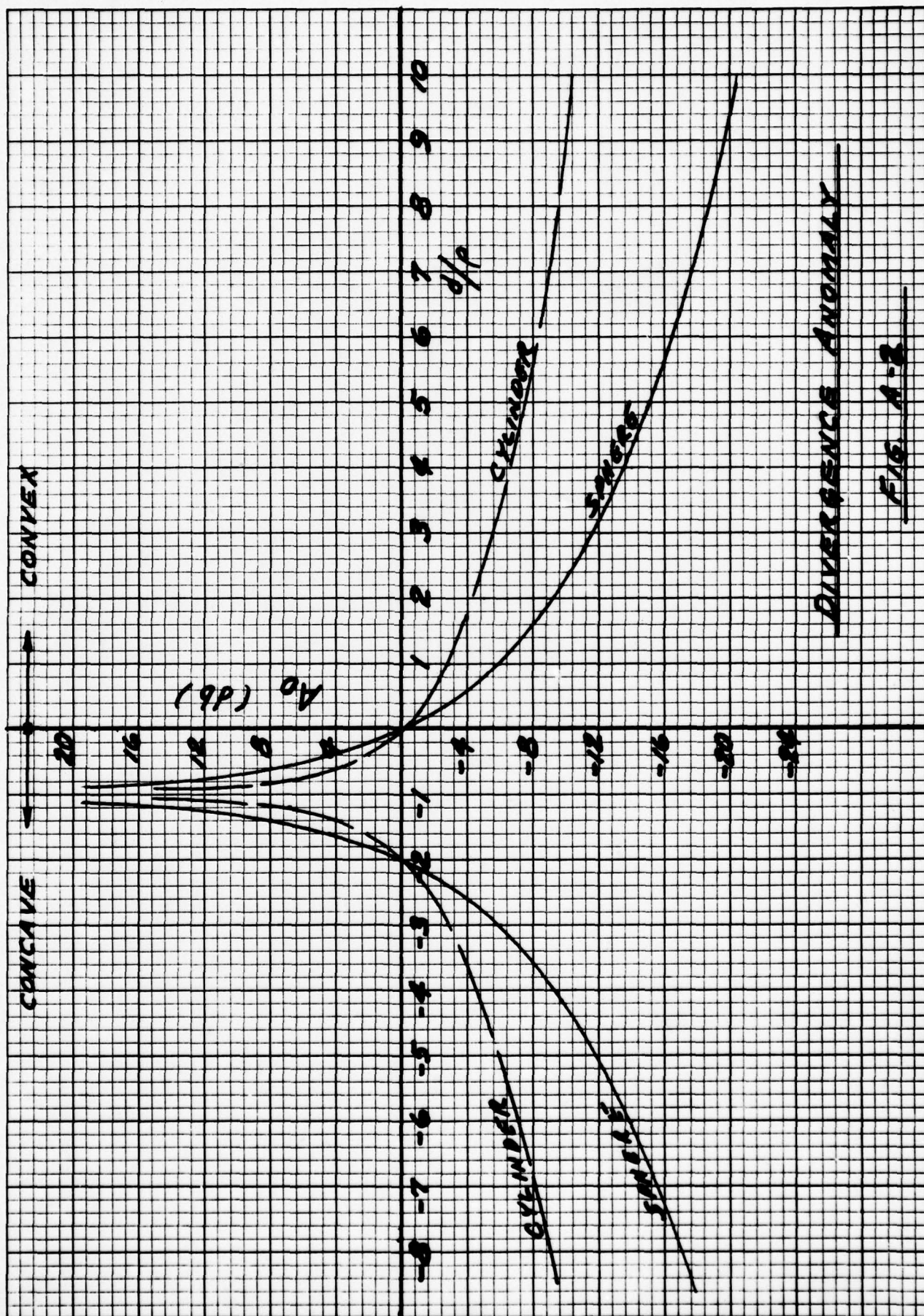
FIG. A-3

III. APPLICATION TO PEARL HARBOR GEOMETRY

The normal incidence tests were conducted in approximately 50' of water with the projector at a depth of 35' and the hydrophone at 43'. Thus $d_1 = 15'$ and $d_2 = 7'$.

From section II, it can be shown that

$$A_{D_c} = \frac{\rho}{\rho + 9.55'}$$

and,

$$A_{D_s} = \left(\frac{\rho}{\rho + 9.55'} \right)^2$$

For cylindrical or spherical surfaces we are then interested in concave surfaces with a radius of curvature more negative than 9.55'.

Figure A-3 shows the value of A_{D_c} and A_{D_s} as a function of ρ. In the cylindrical case, a gain of 5 db occurs when $\rho = 14$ and in the spherical case, when $\rho = 22$.

Figure A-4 shows two typical cross sections of the Wet Slip in Pearl Harbor. The soundings were made with an 11" plate on a sounding line. The two circular arcs show the magnitude of the depressions necessary for a ρ of $-15'$ and $-30'$.

An estimate of the necessary area of this depression can be obtained as follows (see Figure A-5). Focusing occurs primarily during the time in which the beam sweeps out the region between points A and B. The width X is given by

$$X = \left(\frac{r_2^2 + 2\, r_1\, r_2}{4} \right)^{1/2}$$

$$r_2 = ct$$

where,

c is the sound speed

and,

t is the pulse length

This width is conservative for concave surfaces.

-41-
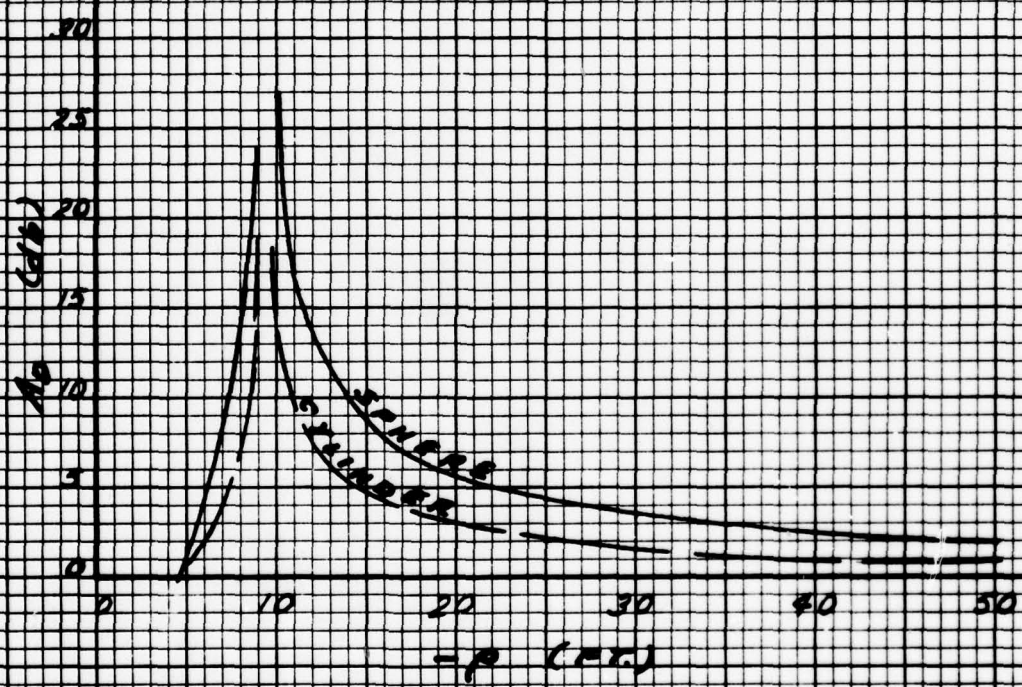
DIVERGENCE ANOMALY
AS RADIUS OF CURVATURE
FOR CONCAVE SURFACE
FIG. A-3
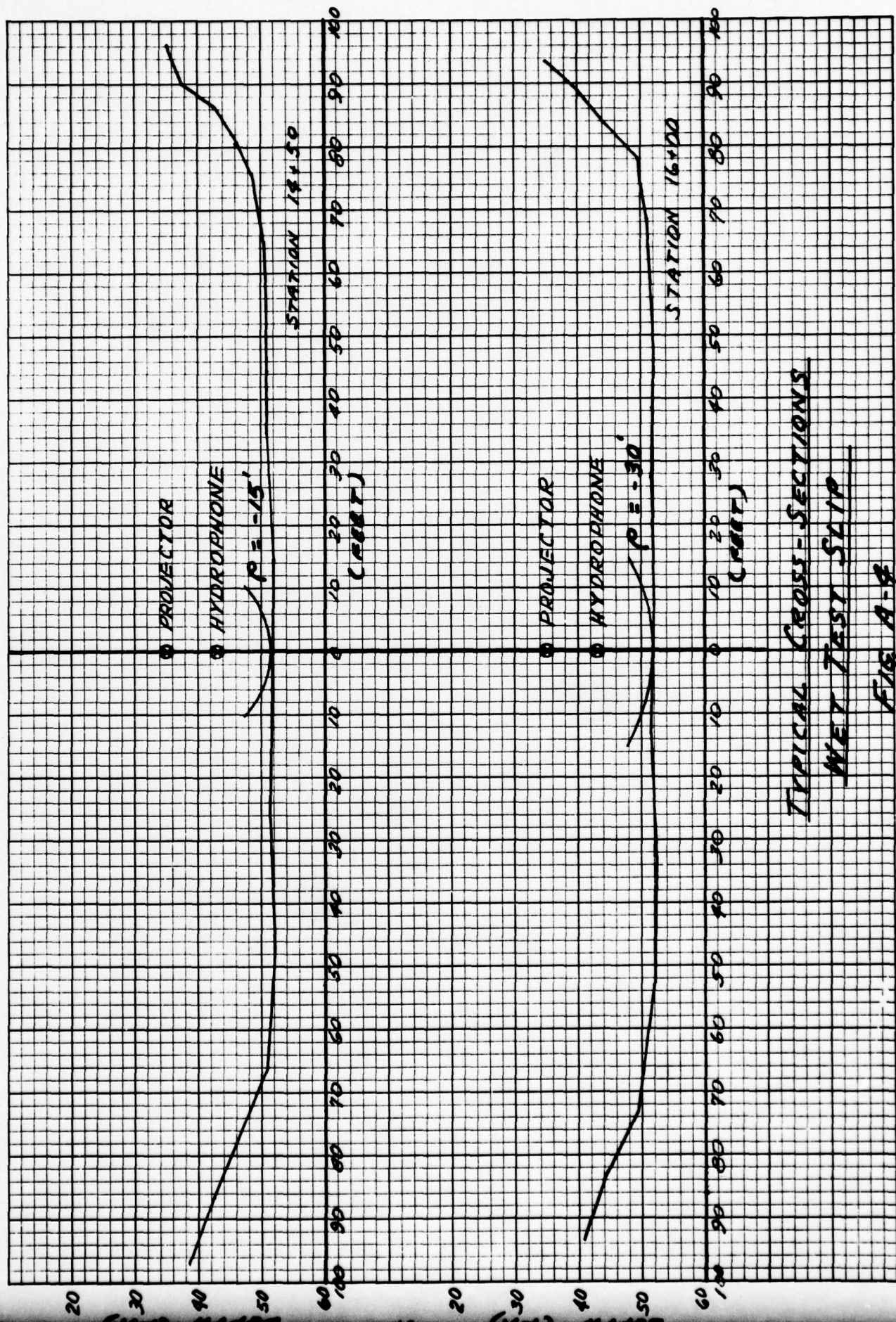
TYPICAL CROSS-SECTIONS

WET TEST SLIP

FIG. A-4
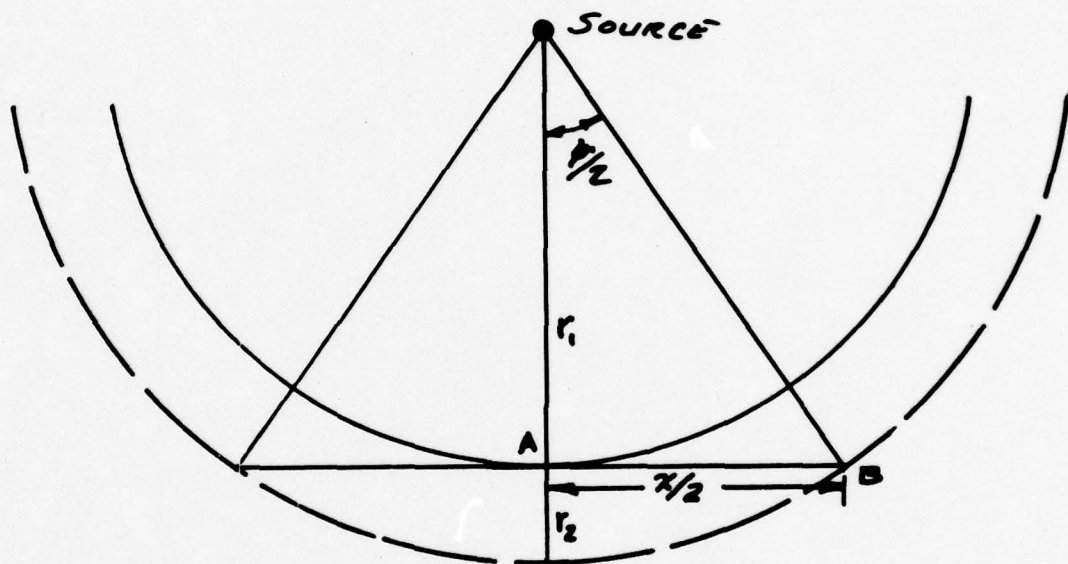
REGION INSONIFIED
BY PULSE LENGTH, t

FIG. A-5

For a pulse length of 2 milliseconds and a sound speed of 5,000 feet/second, the value of X is 10 feet, or $\pm$ 5 feet about the point where sound first reaches the bottom.

Table 1 shows the relief corresponding to the curves shown in Figure A-4.

TABLE I

SURFACE PARAMETERS AS A FUNCTION OF ρ

(in feet)

ρ	X	Z	ΔZ
-30	0	30	0
	5	29.6	0.4
	10	28.3	1.7
	15	26.0	4.0
-15	0	15	0
	5	14.15	0.85
	10	11.2	3.8

It is seen that the bottom depression need only have a depth variation of 0.4' for a $\pm$ 5' horizontal interval for a ρ = -30 and a 0.85' depth variation over a -5' horizontal interval for a ρ of -15.

It seems reasonable to assume that changes in bottom contour of this magnitude could easily exist causing significant changes in the reflected signal. In fact, moving the transducers horizontally a distance of 5 - 10 feet could very possibly change the divergence by an order of magnitude.

PART II

THE EFFECT OF A TWO-LAYER BOTTOM ON
REFLECTION COEFFICIENTS

An attempt has been made to explain some of the variability seen in reflection measurements in Pearl Harbor in terms of a layered bottom. Layering could cause interference effects that would vary the reflection coefficient between a maxima approximately equal to unity (for a pressure release interface) and $-\infty$ for the case of perfect destructive interference. In practice one would expect somewhat more conservative extremes.

Figure A-6 shows the test geometry as constructed from core 73 and the test log book. A water column of 51.5 feet overlays a clay bottom that extends 8.4 feet below the water column and then contacts a hard limestone and coral layer. The source is at a depth of 35 feet and the receiver at 43 feet.

The pressure leaving the source is:

$$P_s = P_o \, e^{-i(wt)}$$

and the pressure at the receiver is: (direct wave)

$$P_r = \frac{P_o}{DR-DS} \, e^{-i\left(wt - \frac{2\pi}{\lambda}(DR - DS)\right)}$$

If the reflection coefficient for the first layer (clay) is R_1, then the pressure at the receiver after reflection is:

$$P_{b1} = \frac{P_o \, R_1}{2D-DR-DS} \, e^{-i\left(wt - \frac{2\pi}{\lambda}(2D-DR-DS)\right)}$$

-47-
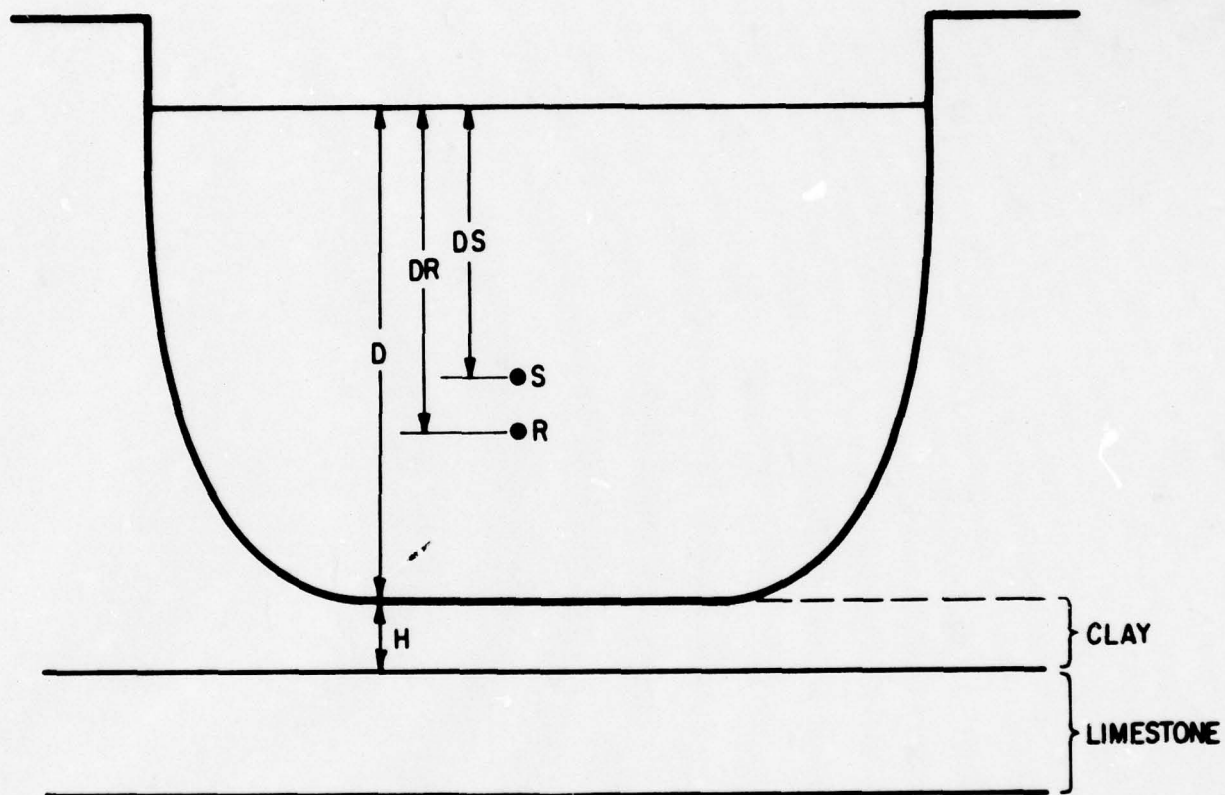
PHNSY WET SLIP GEOMETRY
FIGURE A-6

Similarly, the pressure at the receiver due to the second layer is:

$$P_{b2} = \frac{P_o(1-R_1)(1-R_{01})\,R_2}{2D-DR-DS+2H}\; e^{-i\left[wt-\frac{2\pi}{\lambda}(2D-DR-DS+2H)\right]}$$

where R_2 is the reflection coefficient from the second layer (limestone) and R_{01} is the reflection coefficient for a wave going from the clay layer into the water.

Suppressing the (wt) factor, and realizing that the space wave factor can, in the extreme, cause p_{b1} and p_{b2} to be either in phase or 180° out of phase, the ratio of the direct to the reflected energy is:

$$\left|\frac{p_r}{p_{b2} \pm p_{b1}}\right| = \left|\frac{\dfrac{1}{DR-DS}}{\dfrac{(1-R_1)(1-R_{01})R2}{2D-DR-DS+2H} \pm \dfrac{R_1}{2D-DR-DS}}\right|$$

This ratio includes the effects of spreading loss. The composite pressure reflection coefficient, corrected for the effects of spreading is:

$$R_c = \frac{1}{(1-R_1)(1-R_{01})R_2 \pm R_1}$$

and finally, in DB,

$$\mathcal{R}_c = 20 \log R_c$$

The difference in phase for the two reflected waves is:

$$\Delta\phi = \frac{2\pi}{\lambda}\left[(2D-DR-DS+2H)-(2D-DR-DS)\right]$$

$$\Delta\phi = \frac{2\pi}{\lambda}(2H) = \frac{4\pi fH}{c}$$

-49-

Arthur D. Little, Inc.

where f is the frequency in Hertz and c is the sound speed in the layer H, in cm/sec.

Constructive interference will be a maximum for

$$\Delta\phi = n2\pi \qquad\qquad n = 1,2,3, \ldots\ldots$$

and destructive interference a maximum for

$$\Delta\phi = (2n-1)\pi$$

If H=8.4 feet, f=5000 Hertz and c= 23×10^4 cm/sec., $\Delta\phi$ = 70 degrees. However, a wavelength at this frequency (in clay) is only 1.51 feet long so that the magnitude of $\Delta\phi$ just calculated is relatively unimportant in light of the uncertainties in depth geometry. What is important is that H is about 5.6 wavelengths long which provides adequate length for constructive and destructive interference to occur.

Figure A-7 shows the ratio of the direct pulse to the sum and the difference of the reflected pulses. It should establish approximately the upper and lower bounds for the ratios actually measured from the photographs (before corrections).

Figure A-8 shows the calculated "reflection coefficient" for the two-layer bottom for the cases where the two returns are in phase and 180° out of phase. The corrected data should fall between these two curves.

Assuming a density of 4 gr/cc for limestone, values of reflection coefficient between 5 and 14 db are obtained.

This simple two-layer model, when combined with the divergence concept documented earlier should explain the anomalous appearing Pearl Harbor Data and increase the concern over just how one makes meaningful measurements in shallow water.
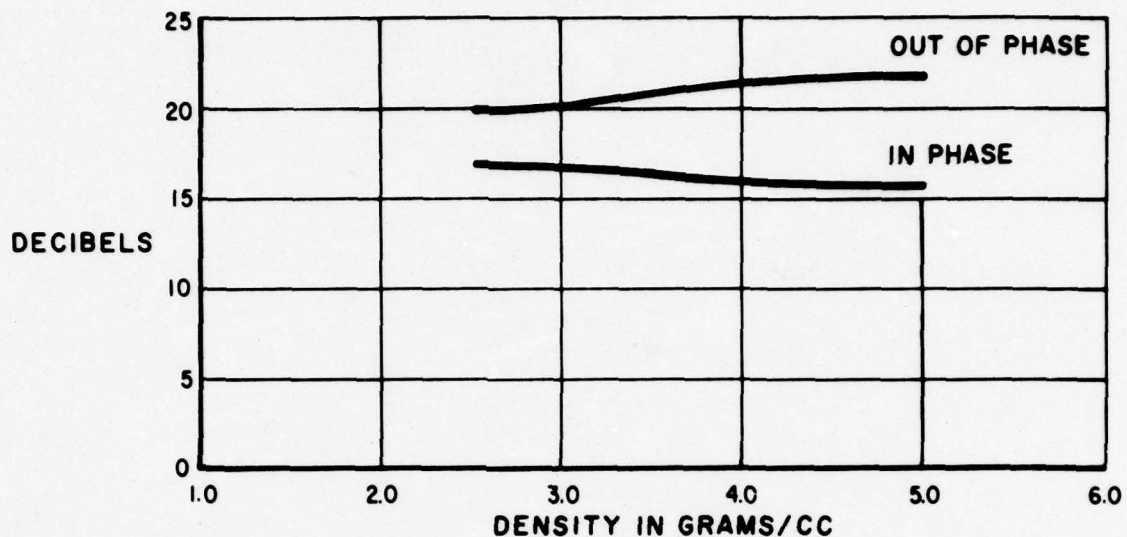
RATIO OF DIRECT PULSE TO
TOTAL REFLECTED PULSE
FIGURE A-7
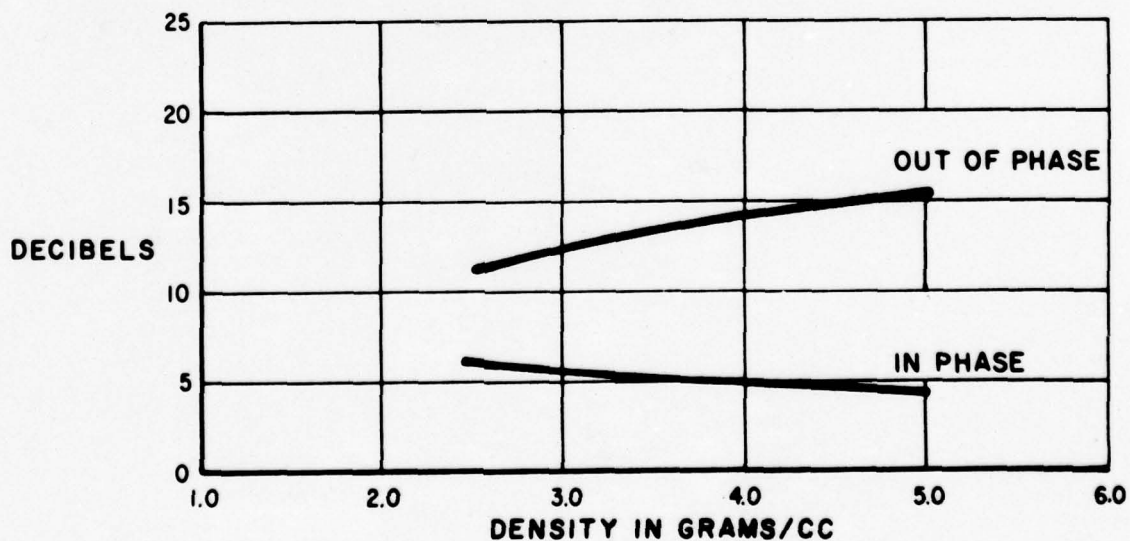
COMPOSITE BOTTOM
REFLECTION COEFFICIENT
FIGURE A-8

-51-

PART III

A SUMMARY OF ENGINEERING PROPERTIES, SEDIMENT SIZE, AND
COMPOSITION ANALYSES OF CORES FROM PEARL HARBOR FOR
ARTHUR D. LITTLE, INC. (MARCH 1967)

Engineering properties
prepared by:
        David Hill

Size and composition
prepared by:
        William Johnson
        John Knoop
        Cary Ross
        Vernon Williams

May 1967

Geological Laboratory Branch
Nearshore Surveys Division
Oceanographic Surveys Department

U. S. Naval Oceanographic Office
Washington, D. C. 20390

CORE ANALYSIS SUMMARY SHEET
SOUND VELOCITY

Analyzed by __Hill__
Date __March 1967__

DEPTH IN CORE (cm)	CORE NO. 1 VELOCITY (F+/sec)	TEMP. (°C)	CORE NO. 2 VELOCITY (F+/sec)	TEMP. (°C)	CORE NO. 3 VELOCITY (F+/sec)	TEMP. (°C)	CORE NO. VELOCITY (F+/sec)	TEMP. (°C)	CORE NO. VELOCITY (F+/sec)	TEMP. (°C)	CORE NO. VELOCITY (F+/sec)	TEMP. (°C)
0	No Reading	*	No Reading	*	No Reading	*						
10	"	*	"	*	"	*						
20	"	*	"	*	"	*						
30	"	*	"	*	"	*						
40	(36) Bottom of core		"	*	"	*						
50			"	*	"	*						
60			"	*	"	*						
70			"	*	"	*						
80			"	*	"	*						
90			"	*	"	*						
100			"	*	"	*						
110			(105) Bottom of core		"	*						
120					"	*						
130					"	*						
140					"	*						
150					"	*						
160					"	*						
170					"	*						
180					"	*						
190					(196) Bottom of core							
200												

* No Reading; obtained due to rocks which distorted the wave making it impossible to make a reading

-54-

EXPLANATION OF DATA PAGES
CORE ANALYSIS SUMMARY SHEET
Engineering Properties
NAVOCEANO (EXP) 3167/18B (Rev. 1-63)

Results of engineering properties, core analysis performed
by the U. S. Naval Oceanographic Office Geological Laboratory are
recorded on Core Analysis Summary Sheet Engineering Properties.

The following is a description of the terms employed on the Core
Analysis Summary Sheet:

1. Cruise Number. A number assigned to each cruise for identi-
fication purposes.

2. Latitude. Expressed in degrees, minutes, and seconds.

3. Longitude. Expressed in degrees, minutes, and seconds.

4. Sample Number. A consecutive number, commencing with 1
applied to each core taken successively throughout the cruise.

5. Date Taken. Day (GMT), month, and year.

6. Water Depth (m). The uncorrected sonic sounding recorded
in meters.

7. Type Corer. Identified by the name of device employed.

8. Core Length (cm). Recorded in centimeters as observed in
the laboratory.

9. Core Penetration (cm). Recorded in centimeters as observed
in the field.

10. Subsample Depth in Core (cm). Interval of subsample as
measured in centimeters from the top of the core.

11. Wet Unit Weight (g/cm^3). The weight (solids plus water)
per unit volume of the sediment mass.

12. Specific Gravity of Solids. The ratio of weight in air of
a given volume of a sediment at 20°C to the weight in air of an equal
volume of distilled water at 20°C.

13. Water Content (% dry weight). The ratio, in percent, of
the weight of water in a given mass of the sediment sample to the
weight of the solid particles.

14. Void Ratio. The ratio of the volume of void spaces to the
volume of solid particles in the sediment sample as computed from
Wet Unit Weight, Specific Gravity of Solids, and Water Content.

15. <u>Saturated Void Ratio</u>. The Void Ratio at 100 percent saturation as computed from Water Content and Specific Gravity of Solids.

$$\text{Saturated Void Ratio} = \frac{\text{Water Content X Specific Gravity of Solids}}{100}$$

16. <u>Porosity (%)</u>. The ratio, usually expressed as a percentage, of the volume of voids of a sediment mass to the total volume of the sediment mass.

17. <u>Liquid Limit</u>. Water Content, in percent, at which a pat of sediment cut by a groove of standard dimension will flow together for a distance of 1/2 inch under the impact of 25 blows in a standard liquid limit apparatus.

18. <u>Plastic Limit</u>. Water Content, in percent, at which a sediment will just begin to crumble when rolled into a thread approximately 1/8 inch in diameter.

19. <u>Plasticity Index</u>. The numerical difference between the Liquid Limit and Plastic Limit of the sediment mass.

20. <u>Liquidity Index</u>. The ratio, expressed in percentage, of (1) the natural water content of the sediment sample minus its Plastic Limit to (2) its Plasticity Index.

21. <u>Compression Index</u>. The slope of the linear portion of the Pressure-Void Ratio curve on a semi-log plot.

22. <u>Compressive Strength</u>. The load per unit area required to shear an unconfined, natural or remolded, sediment mass.

23. <u>Cohesion</u>. The shearing strength per unit area under zero externally applied load.

24. <u>Sensitivity</u>. The ratio of the natural to the remolded strength. It is a measure of the loss of strength due to remolding the sediment mass.

25. <u>Angle of Internal Friction ($^\circ$)</u>. The angle between the abscissa and the tangent of the curve representing the relationship of "shearing resistance" to "normal stress" acting within a sediment mass.

26. <u>Activity</u>. The ratio of the Plasticity Index to the clay fraction percentage ($\ll .002$mm) of the sediment mass.

27. <u>Modulus of Elasticity</u>. The ratio of stress to strain of the sediment mass.

28. <u>Slump (%)</u>. The ratio, in percent, of the amount of height change immediately before the compressive strength test to the original height of a cylinder of sediment.

CORE ANALYSIS SUMMARY SHEET
ENGINEERING PROPERTIES

ANALYZED BY **Hill**

DATE **March 14, 1967**

1. CRUISE NO. A. D. Little & Co.
2. LATITUDE * ___ °
3. LONGITUDE ___ °
4. SAMPLE NO. BS-1
5. DATE TAKEN (Day, month, year) 10/3/67
6. WATER DEPTH (m) Shallow
7. TYPE CORER Hydro plastic
8. CORE LENGTH (cm) 36
9. CORER PENETRATION (cm)

10. SUBSAMPLE DEPTH IN CORE (cm)									
11. WET UNIT WEIGHT (g/cm³)									
12. SPECIFIC GRAVITY OF SOLIDS									
13. WATER CONTENT (% dry weight)									
14. VOID RATIO									
15. SATURATED VOID RATIO									
16. POROSITY (%)									
17. LIQUID LIMIT									
18. PLASTIC LIMIT									
19. PLASTICITY INDEX									
20. LIQUIDITY INDEX									
21. COMPRESSION INDEX FROM LL									
22. COMPRESSIVE STRENGTH NATURAL (g/cm²) REMOLD (g/cm²)									
23. COHESION NATURAL (g/cm²) REMOLD (g/cm²)									
24. SENSITIVITY									
25. ANGLE OF INTERNAL FRICTION (°)									
26. ACTIVITY									
27. MODULUS OF ELASTICITY									
28. SLUMP (%)									

NO ENGINEERING PROPS DUE TO ROCKS AND SHELLS

29. REMARKS * - Core taken near Drydock #3; nearest one to shore.

CORE ANALYSIS SUMMARY SHEET
ENGINEERING PROPERTIES

ANALYZED BY **Hill**

DATE **March 15, 1967**

1. CRUISE NO. **A. D. Little & Co.**
2. LATITUDE ° ' " *
3. LONGITUDE ° ' "
4. SAMPLE NO. **BS - 2**
5. DATE TAKEN (Day, month year) **10/3/67**
6. WATER DEPTH (m) ---
7. TYPE CORER **Hydroplastic**
8. CORE LENGTH (cm) **105**
9. CORER PENETRATION (cm) ---

		0-10	10-20	20-30	30-40	40-50	50-60	60-70	70-80	80-90	90-105
10. SUBSAMPLE DEPTH IN CORE (cm)											
11. WET UNIT WEIGHT (g/cm³)						1.59		1.56			
12. SPECIFIC GRAVITY OF SOLIDS		No		No		2.1		2.65			
13. WATER CONTENT (% dry weight)		65.83			58.99	71.58	78.47	72.89	69.38	85.12	79.64
14. VOID RATIO		EST		EST		2.00	x	1.93			
15. SATURATED VOID RATIO						2.00		1.93			
16. POROSITY (%)						66.67		65.89			
17. LIQUID LIMIT											
18. PLASTIC LIMIT											
19. PLASTICITY INDEX											
20. LIQUIDITY INDEX											
21. COMPRESSION INDEX FROM LL											
22. COMPRESSIVE STRENGTH NATURAL (g/cm²)											
22. COMPRESSIVE STRENGTH REMOLD (g/cm²)											
23. COHESION NATURAL (g/cm²)						-		-			
23. COHESION REMOLD (g/cm²)						-		-			
24. SENSITIVITY						-		-			
25. ANGLE OF INTERNAL FRICTION (°)											
26. ACTIVITY											
27. MODULUS OF ELASTICITY											
28. SLUMP (%)											

29. REMARKS *-Core taken near drydock #3; middle core 0-10,20-30, highly disturbed; 40-50, 60-70-to sloppy, no readings obtained; 80-105-unable to insert vane due to rocks; whole core loaded with shells and rocks. Soil fell apart on touch.

x - Recomputed assuming 100% saturation.

CORE ANALYSIS SUMMARY SHEET
ENGINEERING PROPERTIES

ANALYZED BY __Hill__

DATE __March 15, 1967__

NAVOCEANO-EXP-3162/18-8 (Rev. 1-63)

1. CRUISE NO. A. D. Little & Co.
2. LATITUDE *
3. LONGITUDE
4. SAMPLE NO. BS - 3
5. DATE TAKEN (Day, month, year) 10/3/67
6. WATER DEPTH (m) ---
7. TYPE CORER Hydroplastic
8. CORE LENGTH (cm) 196
9. CORER PENETRATION (cm) ---

	0-10	10-20	20-30	30-40	40-50	50-60	60-70	70-80	80-90	90-100	--100--	110--	120
10. SUBSAMPLE DEPTH IN CORE (cm)													
11. WET UNIT WEIGHT (g/cm³)	No			1.61		1.47			1.56				
12. SPECIFIC GRAVITY OF SOLIDS				2.70		2.32			2.65				
13. WATER CONTENT (% dry weight)	TEST	81.56	78.19	66.96	78.00	82.26	80.17	77.20	84.84	79.88	88.22	86.21	
14. VOID RATIO				1.82 x		1.86			2.15				
15. SATURATED VOID RATIO				1.82		1.90			2.25				
16. POROSITY (%)				64.54		65.03			104				
17. LIQUID LIMIT													
18. PLASTIC LIMIT													
19. PLASTICITY INDEX													
20. LIQUIDITY INDEX													
21. COMPRESSION INDEX FROM LL													
22. COMPRESSIVE STRENGTH NATURAL (g/cm²)													
REMOLD (g/cm²)													
23. COHESION NATURAL (g/cm²)				1.40		2.81							
REMOLD (g/cm²)				—		2.11			—	—			
24. SENSITIVITY				—		1.3							
25. ANGLE OF INTERNAL FRICTION (°)													
26. ACTIVITY													
27. MODULUS OF ELASTICITY													
28. SLUMP (%)													

29. REMARKS * Core taken near drydock #3; furthest from shore 0-10, 110-120, disturbed due to shells and rocks. Soil fell apart on touch.

* Recomputed assuming 100% saturation.

CORE ANALYSIS SUMMARY SHEET
ENGINEERING PROPERTIES

ANALYZED BY __Hill__

DATE __March 15, 1967__

NAVOCEANO-EXP-3167/18-8 (Rev. 1-63)

1. CRUISE NO.							
2. LATITUDE ° ' "							
3. LONGITUDE ° ' "							
4. SAMPLE NO.	BS - 3 (Con't.)						
5. DATE TAKEN (Day, month, year)							
6. WATER DEPTH (m)							
7. TYPE CORER							
8. CORE LENGTH (cm)							
9. CORER PENETRATION (cm)							

	120-130	130-140	140-150	150-160	160-175	175-180	180-190	190-196
10. SUBSAMPLE DEPTH IN CORE (cm)								
11. WET UNIT WEIGHT (g/cm³)		1.52					1.52	
12. SPECIFIC GRAVITY OF SOLIDS		2.70 No			No		2.77 No	
13. WATER CONTENT (% dry weight)	76.50 TEST			96.61	99.49 TEST	92.12	87.40 TEST	
14. VOID RATIO	2.13						2.42 x	
15. SATURATED VOID RATIO	2.06						2.42	
16. POROSITY (%)	68.05						70.76	
17. LIQUID LIMIT								
18. PLASTIC LIMIT								
19. PLASTICITY INDEX								
20. LIQUIDITY INDEX								
21. COMPRESSION INDEX FROM LL								
22. COMPRESSIVE STRENGTH NATURAL (g/cm²)								
REMOLD (g/cm²)								
23. COHESION NATURAL (g/cm²)							2.11	
REMOLD (g/cm²)							—	
24. SENSITIVITY								
25. ANGLE OF INTERNAL FRICTION (°)								
26. ACTIVITY								
27. MODULUS OF ELASTICITY								
28. SLUMP (%)								

29. REMARKS 130-140, 150-160, 160-175, 190-196 - disturbed due to shells and rocks. x - recomputed assuming 100% saturation.

EXPLANATION OF COMPUTER DATA SHEET
SEDIMENT SIZE AND COMPOSITION

Results of sediment-size and composition core analysis performed by the U. S. Naval Oceanographic Office Geological Laboratory are tabulated on Computer Data Sheet Sediment Size and Composition.

The following is an explanation of the terms employed on the Computer Data Sheet:

1. <u>CRUISE.</u> A number assigned to each cruise for identification purposes.

2. <u>SAMPLE.</u> A consecutive number applied to each core taken successively throughout the cruise.

3. <u>LATITUDE.</u> Expressed in degrees, minutes, and tenth of minutes.

4. <u>LONGITUDE.</u> Expressed in degrees, minutes, and tenths of minutes.

5. <u>TAKEN.</u> Date in day, month, and year that core was taken.

6. <u>CORER TYPE.</u> Number corresponding to sampling device code below.

1.	Hydroplastic piston	6.	Orange Peel
2.	Hydroplastic gravity	7.	Ewing
3.	Kullenberg piston	8.	Vibrocorer
4.	Kullenberg gravity	9.	Dredge
5.	Phleger gravity	0.	Other

7. <u>LENGTH.</u> Length of core recorded in centimeters as observed in the laboratory.

8. <u>PENETRATION.</u> Penetration of coring device recorded in centimeters as observed in the field.

9. <u>DEPTH.</u> The uncorrected sonic sounding recorded in meters.

10. <u>ANALYZED.</u> Date in day, month, and year that the core was analyzed in the laboratory.

11. <u>ID. NO.</u> Three digit laboratory project number followed by consecutive number assigned to each subsample analyzed.

12. <u>INTERVAL.</u> Interval of subsample as measured in centimeters from the top of the core.

13. <u>MM.</u> Particle diameter size intervals based on Wentworth size grades in millimeters.

14. <u>PER.</u> Percent of total sample weight within the given size interval. Smallest size analyzed is 0.0010 mm. Percent recorded for 0.0000- is

percentage of particles smaller than 0.0010 mm.

15. GRAVEL, SAND, SILT, CLAY. Percent of total sample weight within the four size classes.

> Class ranges are: Gravel - coarser than 2mm
> Sand   - 2 to 0.0625 mm
> Silt   - 0.0625 to 0.0039 mm
> Clay   - finer than 0.0039 mm

16. MEAN (MM). The geometric mean of the distribution expressed in millimeters.

17. MEAN (PHI). The logarithmic mean of the distribution expressed in phi units ($-\log_2$ of the diameter in millimeters).

18. STAN DEV. Standard deviation. A measure of the degree of spread or dispersion of the distribution about the mean expressed in phi units.

$$s = \sqrt{\sum f(X_1 - \overline{X})^2 / 100}$$

19. SKEWNESS. A measure of the asymmetry of the distribution. Positive values denote skewness of the distribution toward the fine particles, negative values denote skewness toward the coarse particles. A normal distribution has a skewness of 0.

$$SKEWNESS = 1/100 \ 2s^{-3} \sum f(X_1 - \overline{X})^3$$

20. KURTOSIS. A measure of the peakedness of the distribution. Positive values denote a "leptokurtic" distribution, or a distribution more "peaked" than normal. Negative values denote a "platykurtic" distribution, or a distribution more "flat" than normal. A normal curve has a kurtosis of 0.

$$KURTOSIS = 1/100 \ s^{-4} \sum f(X_1 - \overline{X})^4 - 3$$

21. $CACO_3$. Percent calcium carbonate of the total sample weight as determined by the insoluble residue method.

22. ORG CARBON. Percent organic carbon of the total sample weight as determined by the Allison method.

23. COLOR. Wet sediment color, based on the Geological Society of America Rock-Color Chart, as determined in the laboratory.

24. DOM MINERAL. Dominant mineral (s) comprising the sample assemblage.

25. SEC MINERAL. Secondary mineral (s) comprising the sample assemblage.

SEDIMENT SIZE AND COMPOSITION DATA

CRUISE TITLE
CORER TYPE 2   SAMPLE 1   LENGTH 36.0   LATITUDE 0 0.0   PENETRATION 0.0   LONGITUDE 0 0.0   DEPTH 0.0   TAKEN 10/03/67   ANALYZED 14/03/67

BOX NO.	308 6	308 7	308 8
INTERVAL	0.0- 5.0	14.0- 20.0	30.0- 36.0
MM	PER	PER	PER
4.0000	0.000	31.884	33.459
2.0000	0.082	10.870	23.183
1.0000	0.082	13.043	9.273
0.5000	0.409	7.971	5.639
0.2900	3.273	5.072	3.133
0.1250	13.093	3.623	2.882
0.0625	11.047	2.536	2.005
0.0312	10.229	7.971	6.767
0.0156	5.319	0.362	0.877
0.0078	4.910	0.362	0.627
0.0039	15.912	5.072	1.880
0.0020	8.592	2.899	4.010
0.0010	10.638	2.899	2.130
0.0005	0.000	0.000	0.000
0.0000-	18.412	5.435	4.135
GRAVEL	0.082	42.754	56.642
SAND	27.905	32.246	22.932
SILT	34.370	13.768	10.150
CLAY	37.643	11.232	10.276
MEAN (MM)	0.0094	0.4355	0.6877
MEAN (PHI)	6.7373	1.1993	0.5401
STAN DEV	3.2553	4.2580	4.0126
SKEWNESS	0.0182	0.6206	0.8069
KURTOSIS	-1.2588	-0.1366	0.7709
CACO3	77.400	91.800	89.000
ORG CARBON	0.000	0.000	0.000
COLOUR	N4	N4	N4
DOM MINERAL	SHELL	SILT	SILT
SEC MINERAL	CLAY	SHEL DK MI	SHELL

SEDIMENT SIZE AND COMPOSITION DATA

| CRUISE LITTLE | SAMPLE 2 | LATITUDE 0 0.0 | LONGITUDE 0 0.0 | TAKEN 10/03/67 |
| CORER TYPE 2 | LENGTH 105.0 | PENETRATION 105.0 | DEPTH 0.0 | ANALYZED 15/03/67 |

| BOJ NO. | 308 1 | 308 2 | 308 3 | 308 4 | 308 5 |
| INTERVAL | 0.0- 10.0 | 40.0- 50.0 | 60.0- 70.0 | 80.0- 90.0 | 100.0-105.0 |

MM	PER	PER	PER	PER	PER
4.0000	23.220	9.827	3.679	24.458	12.040
2.0000	13.932	4.913	6.020	2.788	3.679
1.0000	6.192	2.890	3.344	3.096	3.679
0.5000	4.334	2.601	3.010	3.096	3.010
0.2500	3.096	2.023	2.676	2.167	2.676
0.1250	2.788	2.312	2.676	2.788	3.010
0.0625	0.619	2.023	0.334	2.477	2.676
0.0312	8.978	34.104	32.776	8.669	21.739
0.0156	4.334	3.468	6.355	4.954	2.676
0.0078	3.715	5.780	2.007	8.050	5.686
0.0039	8.050	6.069	4.013	8.978	8.027
0.0020	4.644	7.225	9.365	8.050	8.696
0.0010	1.548	3.468	5.351	8.050	5.351
0.0005	0.000	0.000	0.000	0.000	0.000
0.0000-	14.591	13.295	18.395	12.384	17.057

GRAVEL	37.152	14.740	9.699	27.245	15.719
SAND	17.028	11.850	12.040	13.622	15.050
SILT	25.077	49.422	45.150	30.650	38.127
CLAY	20.743	23.988	33.110	28.483	31.104
MEAN (MM)	0.1214	0.0343	0.0205	0.0519	0.0281
MEAN (MMD)	3.0418	4.8671	5.6104	4.2678	5.1555
STAN DEV	5.1070	4.1512	4.0939	5.0082	4.5439
SKEWNESS	0.2306	-0.0648	-0.0818	-0.0416	-0.1077
KURTOSIS	-1.4680	-0.8768	-0.8768	-1.6159	-1.1937
CACO3	70.200	47.100	39.900	63.300	53.900
ORG CARBON	0.000	0.000	0.000	0.000	0.000
COLOR	5Y4/1	5Y4/1	5Y4/1	5Y4/1	5Y4/1
DOM MINERAL	SILT	SILT	SHELL	SHELL	SHELL
SEC MINERAL	SHELL	SHELL	DK MINERAL	DK MINERAL	DK MINERAL

SEDIMENT SIZE AND COMPOSITION DATA

CRUISE KITRUE CORER TYPE 2 SAMPLE 3 LATITUDE 0 0.0 LONGITUDE 0 0.0 TAKEN 10/03/67
LENGTH 196.0 PENETRATION 0.0 DEPTH 0.0 ANALYZED 15/03/67

ID NO.	308 9	308 10	308 11	308 12	308 13	308 14
INTERVAL	0.0-10.0	30.0-40.0	50.0-60.0	90.0-90.0	110.0-120.0	120.0-130.0
MM	PER	PER	PER	PER	PER	PER
4.00000	0.000	0.000	7.605	0.000	11.111	4.394
2.00000	9.955	3.559	5.323	1.757	6.061	1.757
1.00000	3.167	2.491	2.281	1.767	3.030	3.076
0.5000	2.713	2.491	2.662	1.767	3.030	2.636
0.2500	2.262	2.491	3.042	2.120	3.030	3.515
0.1250	2.715	3.203	4.183	3.534	4.040	4.833
0.0625	0.905	3.203	2.662	3.534	1.684	4.394
0.0312	20.814	24.955	7.224	21.201	12.121	25.483
0.0156	3.420	2.135	3.802	2.827	3.704	3.954
0.0078	8.145	4.270	7.224	4.947	5.051	7.469
0.0031	9.955	6.406	11.027	9.187	5.387	13.181
0.0020	10.860	10.320	12.928	8.834	10.774	14.060
0.0010	5.430	5.694	4.943	6.360	5.724	7.909
0.0005	0.000	0.000	0.000	0.000	0.000	0.000
0.0000-	19.457	29.181	25.095	32.155	25.253	3.339
GRAVEL	9.955	3.559	12.928	1.767	17.172	6.151
SAND	11.765	13.879	14.829	12.721	14.815	18.453
SILT	42.934	37.367	29.278	38.163	26.263	50.088
CLAY	35.747	45.196	42.966	47.350	41.751	25.308
MEAN (QM)	0.0149	0.0082	0.0130	0.0060	0.0195	0.0244
MEAN (PHI)	6.0701	6.9306	6.2605	7.3905	5.5818	5.3576
STAN DEV	4.0685	3.8628	4.5746	3.6312	4.9169	3.3439
SKEWNESS	-0.1882	-0.1767	-0.2739	-0.2048	-0.1640	-0.2560
KURTOSIS	-0.8380	-0.8939	-1.0053	-0.8308	-1.3577	-0.4070
CACO3	40.000	39.800	37.600	33.400	40.900	32.000
ORG CARBON	0.000	0.000	0.000	0.000	0.000	0.000
COLOR	5Y5/2	5Y5/2	5Y5/2	5Y5/2	5Y5/2	5Y5/2
DOM MINERAL	SILT	CLAY	CLAY	CLAY	CLAY	SILT
SEC MINERAL	SHEL DK MI	SHELL	SHELL	SHEL DK MI	SHELL	SHEL DK P

IDA NO.	308 16			308 17			
INTERVAL	180.0-190.0			190.0-196.0			
MM	PER	PER	PER	PER	PER	PER	PER
4.0000	9.125			2.518			
2.0000	3.422			2.878			
1.0000	1.521			1.439			
0.5000	2.281			2.158			
0.2500	2.281			2.518			
0.1250	3.422			3.597			
0.0625	1.521			3.597			
0.0312	8.745			37.410			
0.0156	6.084			3.957			
0.0078	9.125			3.237			
0.0039	10.644			6.475			
0.0020	12.167			8.273			
0.0010	10.266			7.554			
0.0005	0.000			0.000			
0.0000-	19.392			14.388			
GRAVEL	12.548			5.396			
SAND	11.027			13.309			
SILT	34.601			51.079			
CLAY	41.825			30.216			
MEAN (MM)	0.0131			0.0177			
MEAN (PHI)	6.2547			5.8237			
STAN DEV	4.3726			3.5558			
SKEWNESS	-0.3305			-0.0494			
KURTOSIS	-0.7529			-0.4703			
CACO3	0.000			46.300			
ORG CARBON	0.000			0.000			
COLOR	5Y5/2			5Y5/2			
DOM MINERAL	CLAY			SILT			
SEC MINERAL	SWEL DK M1			SWEL DK M1			

PART IV

NAVAL RESEARCH LABORATORY
UNDERWATER SOUND REFERENCE DIVISION
P. O. BOX 8337
ORLANDO, FLORIDA 32806

IN REPLY REFER TO:
8205
S02-31(ADLittle)
Ser 250-67
6 April 1967

Arthur D. Little, Inc.
35 Acorn Park
Cambridge, Mass.   02140

Attention: Mr. George E. Miller

Gentlemen:

The enclosed prints USRD 48222 through 48228 and 45001
show the vertical directivity of hydrophones type CH-1A.
They are forwarded for the information of
Mr. George E. Miller as requested by him during a tele-
phone conversation with Mr. Ward Paine on 22 March 1967.

Very truly yours,

D. T. Hawley

D. T. HAWLEY
Chief Scientist (Acting)
Underwater Sound Reference Division
By direction of the Director

-68-

COORDINATE SYSTEM FOR TRANSDUCER ORIENTATION

The left-handed coordinate system of the American Stand-
ard Procedures for Calibration of Electroacoustic Trans-
ducers Particularly Those for Use in Water, Z24.24-1957,
is used. The transducer is fixed with respect to the
coordinate system and has its acoustic center at the
origin. The angle ϕ is equivalent to the azimuth angle
in sonar operation.
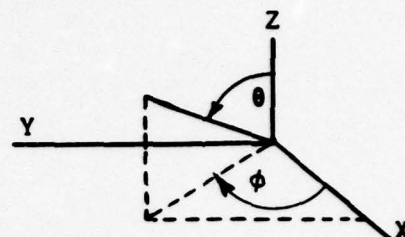
PLACEMENT OF TRANSDUCER IN COORDINATE SYSTEM

Transducer Type	Transducer Orientation in Coordinate System
Point, or Spherical	Points on surface that coincide with the X and Z axes shall be specified.
Cylindrical, or Line	The axis of the cylinder or line shall coincide with the Z axis. A reference mark in the XZ plane and in the direction of the positive X axis will be specified.
Plane, or Piston	The plane or piston face shall be in the YZ plane with the X axis normal to the face at its acoustic center. A reference mark in the XZ plane and in the direction of the positive Z axis will be specified.
Other Configu-rations	Orientation shall be shown by sketch or description. This category includes line and piston types of transducers operated in an orientation other than those specified above.

ORIENTATIONS FOR RESPONSE AND DIRECTIVITY MEASUREMENTS

Response. The calibration measurements are made for sound propagated parallel to the
positive X axis ($\phi = 0$, $\theta = 90$), unless otherwise specified on the response curve.

Directivity. The plane of the pattern is specified, and the following conventions are
observed, if another orientation is not specified on the pattern:

XY Plane: The positive X axis ($\phi = 0$, $\theta = 90$) coincides with the zero-degree direction on
the pattern and the positive Y axis ($\phi = 90$, $\theta = 90$) is at 90 degrees measured
in a clockwise direction. Rotation is around the Z axis; the positive Z axis
is directed upward from the plane of the paper.

XZ Plane: The positive X axis coincides with the zero-degree direction and the positive
Z axis ($\theta = 0$) is at 90 degrees measured in a clockwise direction. Rotation is
around the Y axis; the negative Y axis is directed upward from the plane of the
paper.

YZ Plane: The positive Y axis coincides with the zero-degree direction and the positive
Z axis is at 90 degrees measured in a clockwise direction. Rotation is around
the X axis; the positive X axis is directed upward from the plane of the paper.

MEASUREMENTS MADE IN AC-
CORDANCE WITH AMERICAN
STANDARD Z24.24-1957

Relative Response in dB

10

20

30

40

30°
330°

20°
340°

10°
350°

0°

350°
10°

340°
20°

330°
30°

40°
320°

330°
30°

50°
310°

310°
50°

60°
300°

300°
60°

70°
290°

290°
70°

80°
280°

280°
80°

90°
270°

270°
90°

100°
260°

260°
100°

110°
250°

250°
110°

120°
240°

240°
120°

130°
230°

23
13

140°
220°

cable

DIRECTIVITY
Ch-1A Hydrophone
Serial 2056
XZ plane

3.5 kHz

DIVISION NRL

USN UNDERWATER SOUND REFERENCE LABORATORY
P O BOX 8337   ORLANDO, FLA. 32806

150°

160°

170°

180°

190°

200°

210°

USRD NO.48223

PROJECT NO. 19N87

DATE: Mar 1967

MEASUREMENTS MADE IN AC-
CORDANCE WITH AMERICAN
STANDARD 724 24-1957

DIRECTIVITY
Ch-1A Hydrophone
Serial 2056
XZ plane

5.0 kHz

DIVISION, NRL

USN UNDERWATER SOUND REFERENCE LABORATORY

P O BOX 8337   ORLANDO, FLA. 32806

USRD NO. 48224

PROJECT NO. 19N67

DIRECTIVITY
CH-1A Hydrophone
Serial 2056
XZ plane

6.4 kHz

DIVISION NRL

USN UNDERWATER SOUND REFERENCE LABORATORY

P O BOX 8337   ORLANDO, FLA. 32806

Relative Response in dB

USRD NO. 48225

PROJECT NO. 1GNS7

DATE: Mar 1967

MEASUREMENTS MADE IN AC-
CORDANCE WITH AMERICAN
STANDARD Z24.24-1957

DIRECTIVITY
CH-1A Hydrophone
Serial 2056
XZ plane

8.0 kHz

DIVISION, NRL

USN UNDERWATER SOUND REFERENCE LABORATORY
P O BOX 8337   ORLANDO, FLA. 32806

USRD NO. 48226

PROJECT NO. 19N67

DATE: Mar 1967

MEASUREMENTS MADE IN AC
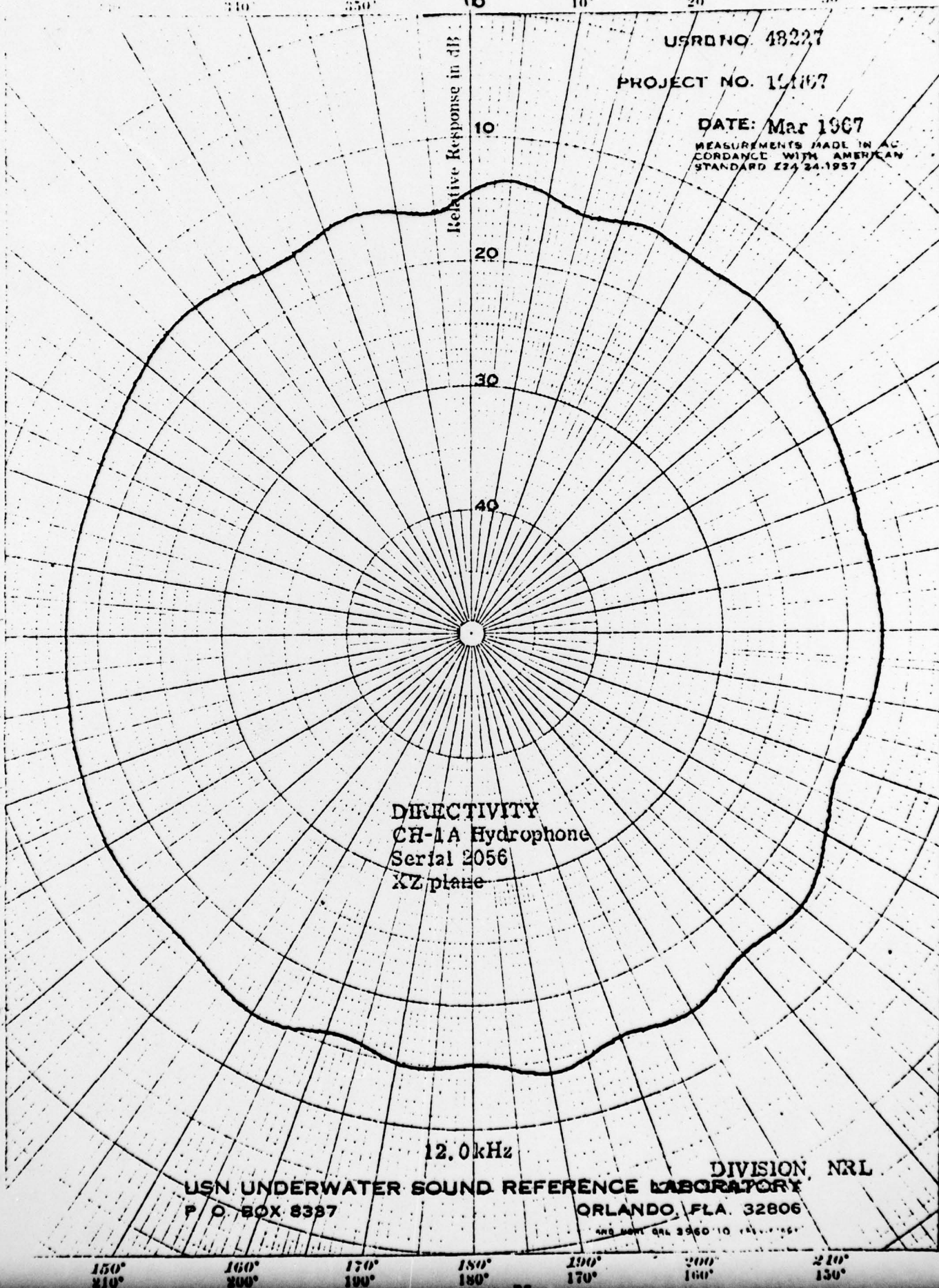CORDANCE WITH AMERICAN
STANDARD Z24.24-1957

Relative Response in dB

DIRECTIVITY
CH-1A Hydrophone
Serial 2056
XE plane

10.0 kHz

DIVISION, NRL
USN UNDERWATER SOUND REFERENCE LABORATORY
P. O. BOX 8337   ORLANDO, FLA. 32806

Relative Response in dB

USRD NO. 48227

PROJECT NO. 1-167

DATE: Mar 1967

MEASUREMENTS MADE IN AC-
CORDANCE WITH AMERICAN
STANDARD Z24.24-1957

0 db

10

20

30

40

DIRECTIVITY
CH-1A Hydrophone
Serial 2056
XZ plane

12.0 kHz

DIVISION NRL

USN UNDERWATER SOUND REFERENCE LABORATORY

P O BOX 8337

ORLANDO, FLA. 32806

USRD NO. 48228

PROJECT NO. 19N67

DATE: Mar 1967

MEASUREMENTS MADE IN AC
CORDANCE WITH AMERICAN
STANDARD Z24.24-1957

Relative Response in dB

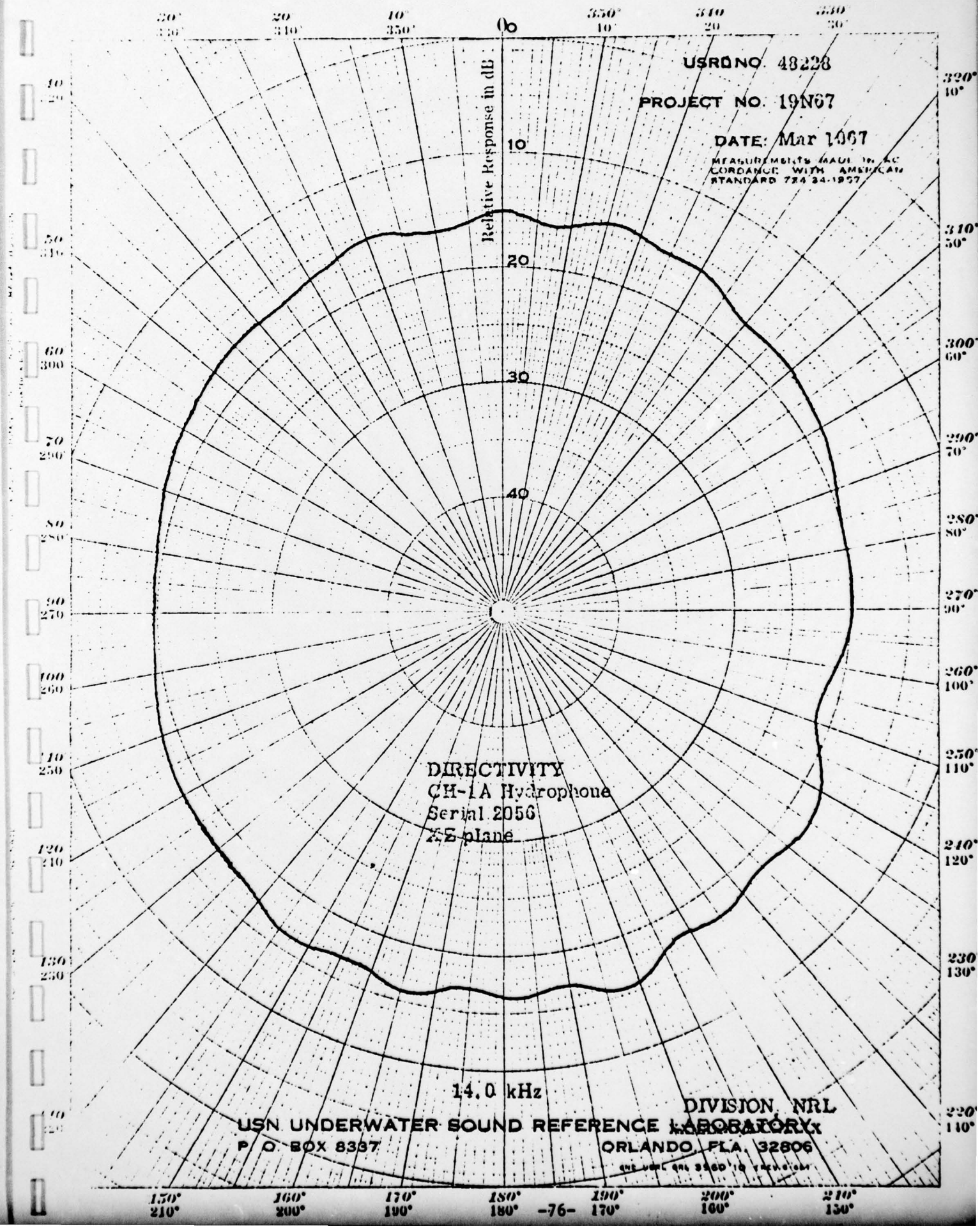DIRECTIVITY
CH-1A Hydrophone
Serial 2056
XZ plane

14.0 kHz

DIVISION, NRL

USN UNDERWATER SOUND REFERENCE LABORATORY
P. O. BOX 8337   ORLANDO, FLA. 32806

-76-